Title: Large-Scale Structure with 21cm Intensity Mapping

Date: Nov 13, 2018 11:00 AM

URL: http://pirsa.org/18110083

Abstract: <p>In this talk I will discuss several aspects of using the 21cm Intensity Mapping (IM) as a Large-Scale Structure (LSS) probe in order to better constrain the cosmological parameters. I will start with a Baryon Acoustic Oscillations (BAO) reconstruction method intended for 21cm IM observations at low redshifts. I will then present the predictions and gains of performing 21cm IM surveys at redshift range which is currently vastly unobserved (2<z<6). Finally I will show the results of using existing data (ALFALFA & SDSS) to place constraints on the distribution of neutral hydrogen (HI) in dark matter halos as a function of the halo mass. This is then used to constrain and improve the HI halo model needed to make accurate and precise predictions on the 21cm signal and the noise.</p>

UNIVERSITY OF WATERLOO

Cosmology and Gravitation Seminar

Large-Scale Structure with 21cm Intensity Mapping

Andrej Obuljen

New postdoc at UWaterloo working with Will Percival
Associate Postdoc at PI

Nov 13th 2018

Origins

From Belgrade (Serbia)
PhD studies at SISSA (Trieste, Italy)

SISSA 40!

INFN

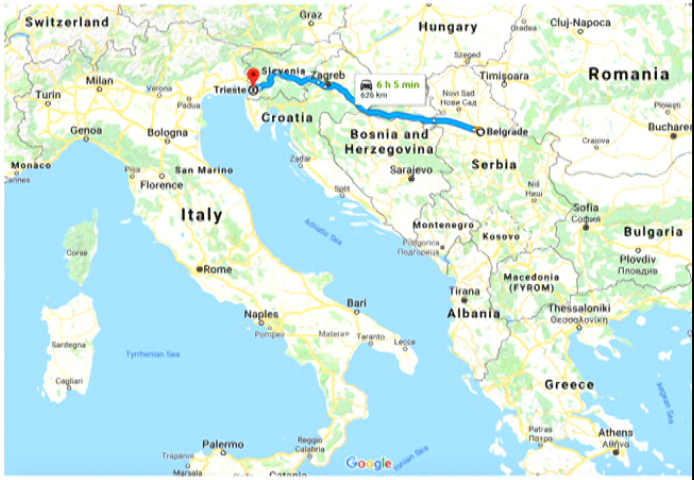

PhD supervisor: Matteo Viel (SISSA)

Collaborated with:
Francisco Villaescusa-Navarro (CCA)
Emanuele Castorina (BCCP)
David Alonso (Oxford) et al.

Part of:
Cosmic Visions 21cm Collaboration Group
DESI

Outline

- Introduction — Baryon Acoustic Oscillations — 21cm cosmology
- BAO reconstruction with pixels
- High-redshift post-reionization cosmology with 21cm intensity mapping
- The HI content of dark matter haloes at $z \approx 0$ from ALFALFA
- Summary & future work

Introduction

- We are witnessing exciting times in the field of cosmology
- We have a well-established 6-parameter model (ΛCDM) that describes well many observables at different times, energies and scales
- We have measured most of these parameters with sub-percent precision
- We have learned most of this using:
  - Anisotropies in the Cosmic Microwave Background (CMB) radiation
  - Galaxy clustering
  - Measurements of distances to 'local' Supernovae Ia
  - Weak lensing
  - Ly-a forest

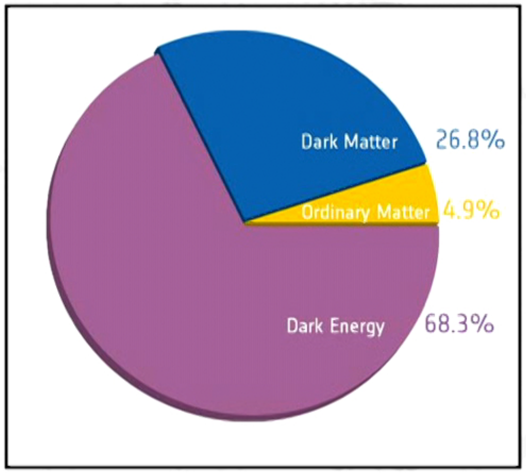

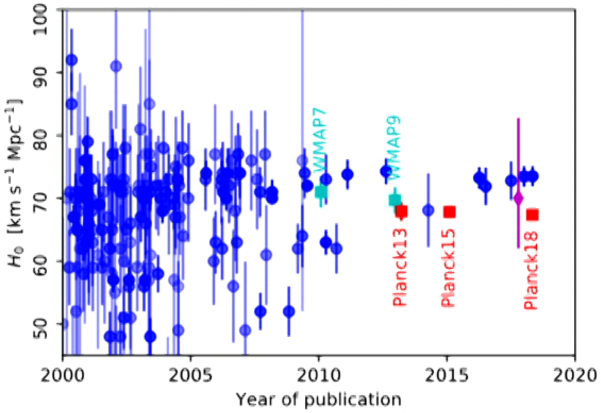

Planck collaboration

Correlation function/Power spectrum

$$\langle \delta(\vec{x}_1)\,\delta(\vec{x}_2)\rangle \equiv \xi(r_{12})$$

$$\left\langle \delta(\vec{k}_1)\delta^*(\vec{k}_2)\right\rangle \equiv (2\pi)^3\delta_{\rm D}(\vec{k}_1+\vec{k}_2)P(k_1)$$

CMB

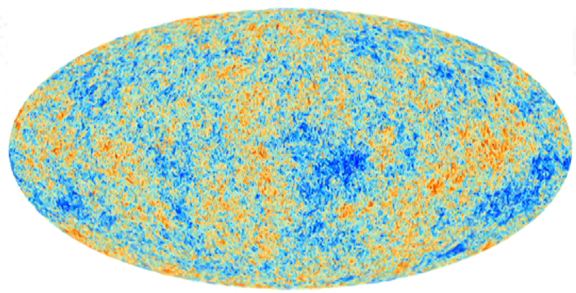

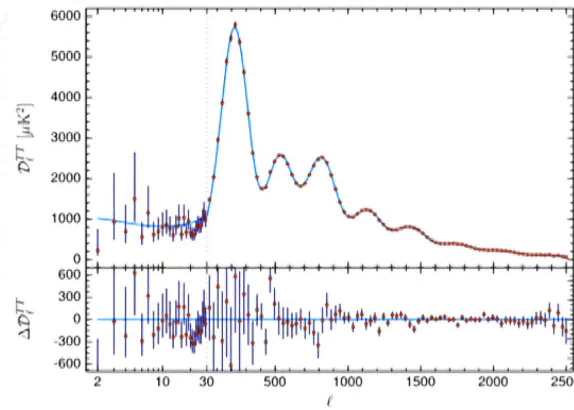

LSS

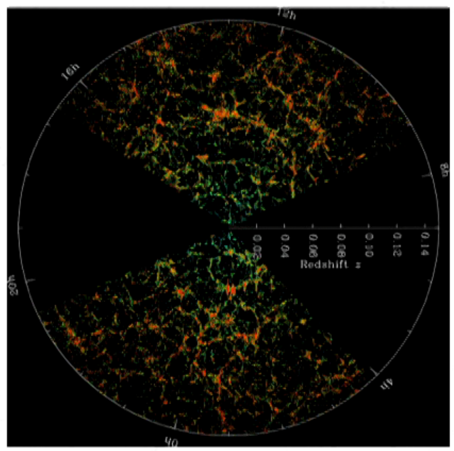

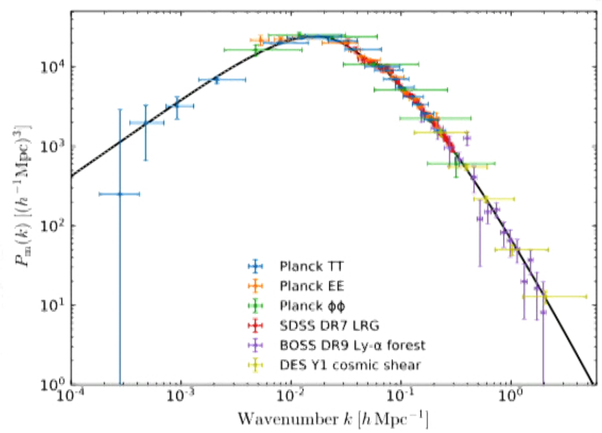

SDSS

Planck collaboration, 2018

Baryon Acoustic Oscillations (BAO)

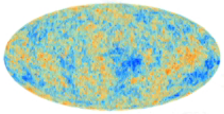

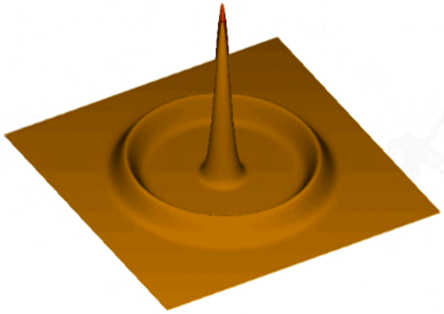

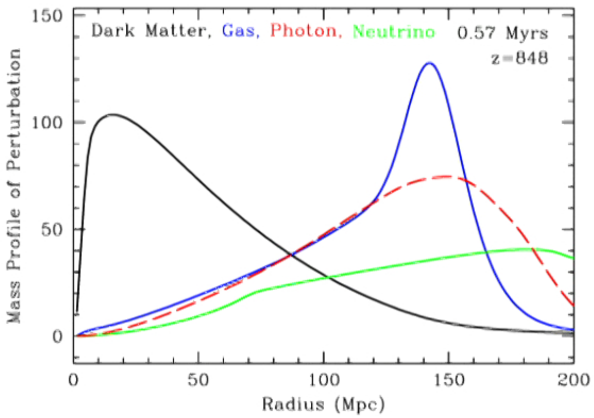

Eisenstein et al, 2005,2007

Baryon Acoustic Oscillations (BAO)

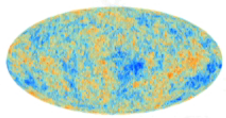

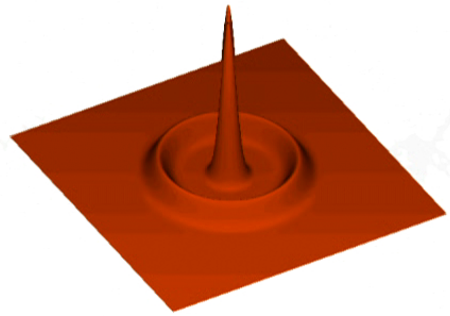

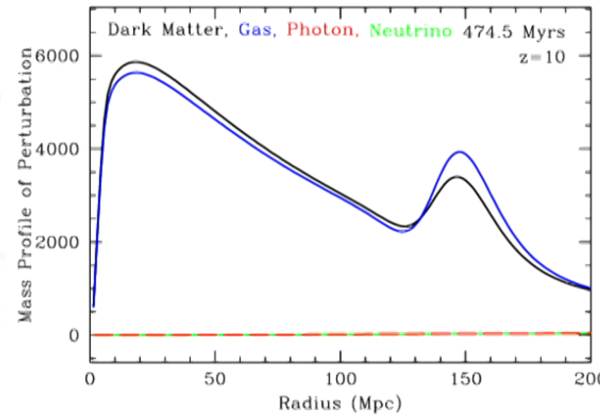

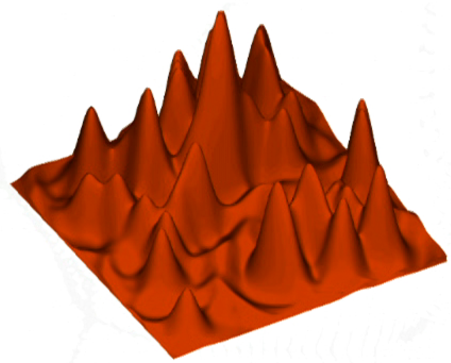

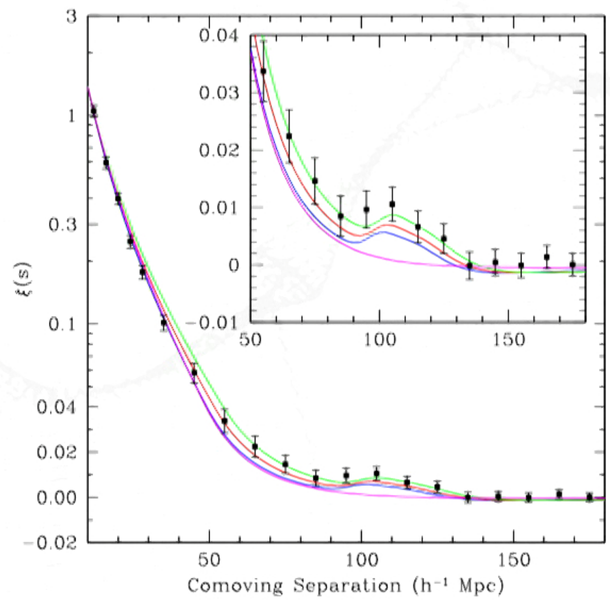

Eisenstein et al, 2005,2007

Expansion history with BAO

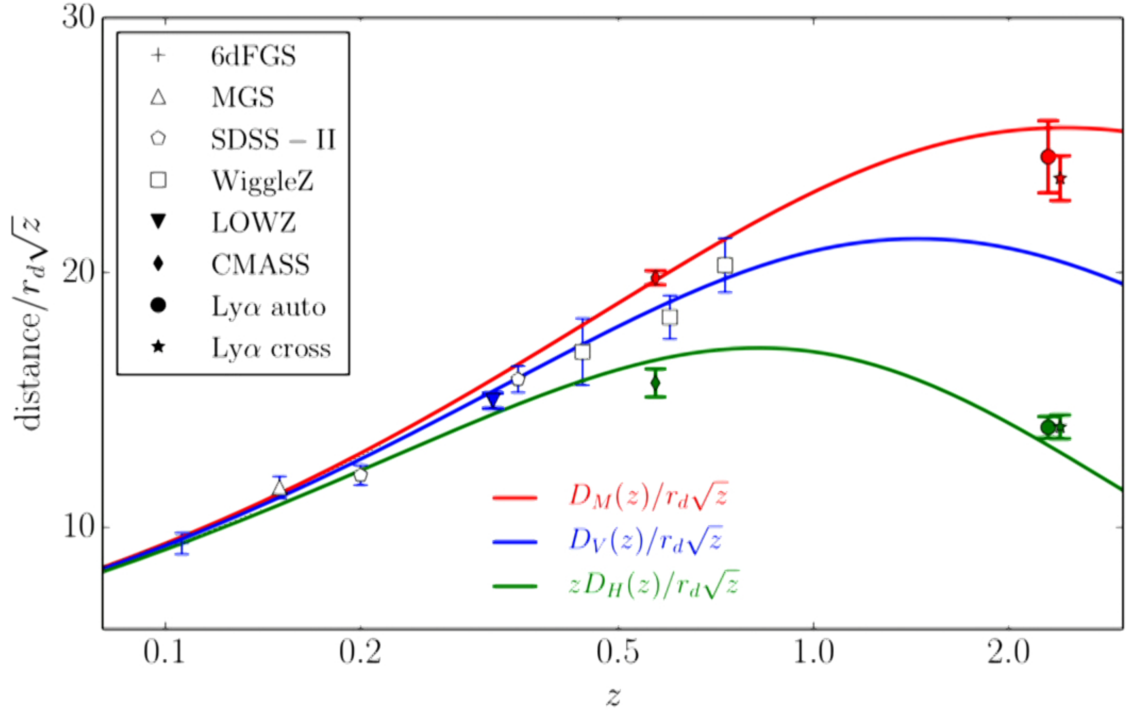

Aubourg et al, 2015

Non-linear effects on BAO

Large scale movements of galaxies cause the BAO peak to broaden

Dominant effect comes from coherent flows of galaxies, rather than random motions

BAO scale is in mildly non-linear regime, and we can model and undo these flows using Zel'dovich approximation

Introduces a shift in BAO peak ~ 0.3%

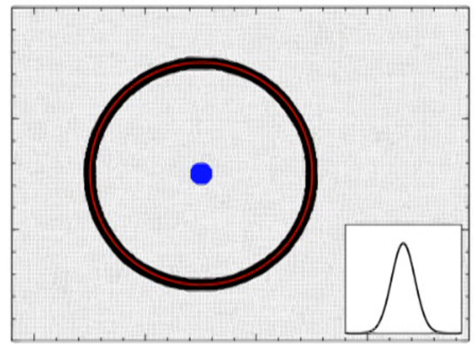

Padmanabhan et al, 2012

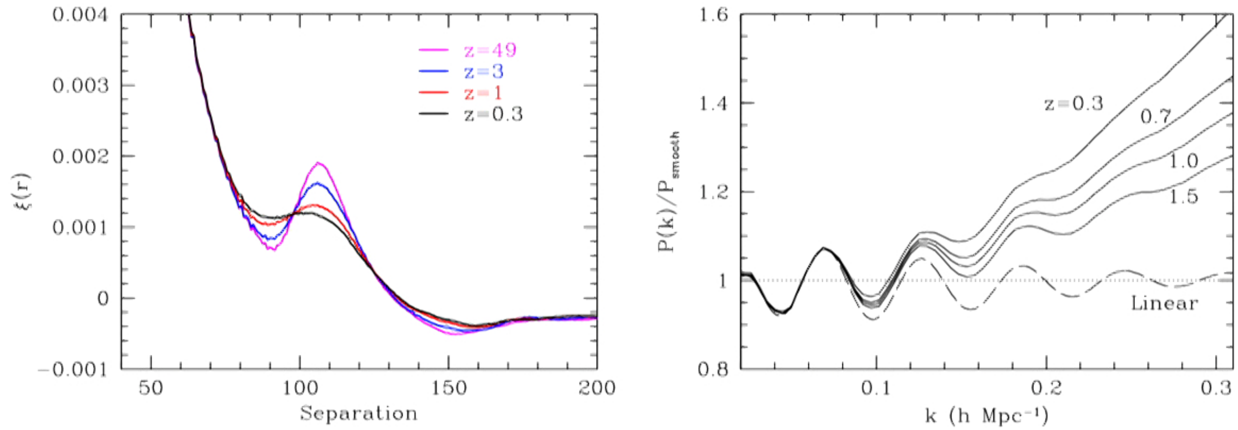

Weinberg, D. H. et al, 2013

Non-linear effects on BAO

Large scale movements of galaxies cause the BAO peak to broaden

Dominant effect comes from coherent flows of galaxies, rather than random motions

BAO scale is in mildly non-linear regime, and we can model and undo these flows using Zel'dovich approximation

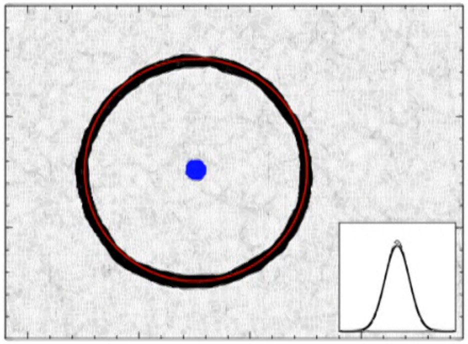

Padmanabhan et al, 2012

Introduces a shift in BAO peak ~ 0.3%

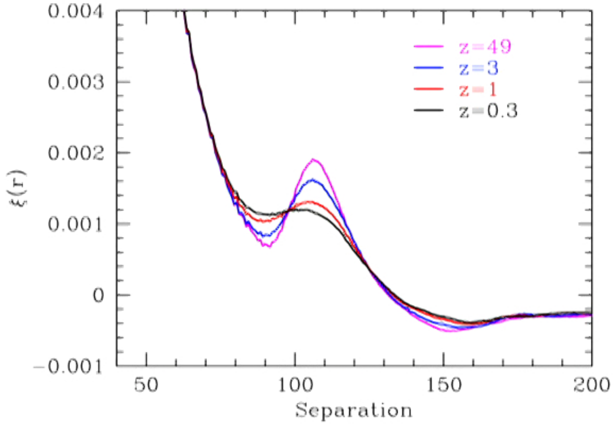

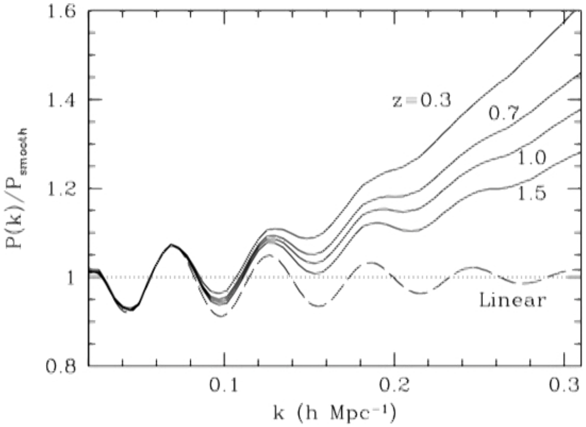

Weinberg, D. H. et al, 2013

Neutral hydrogen (HI)

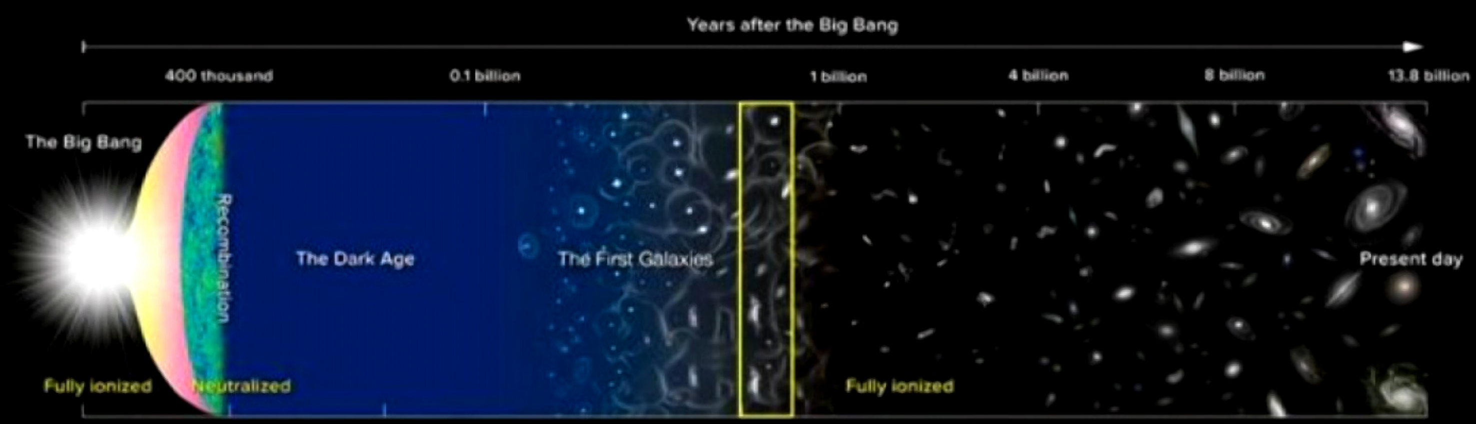

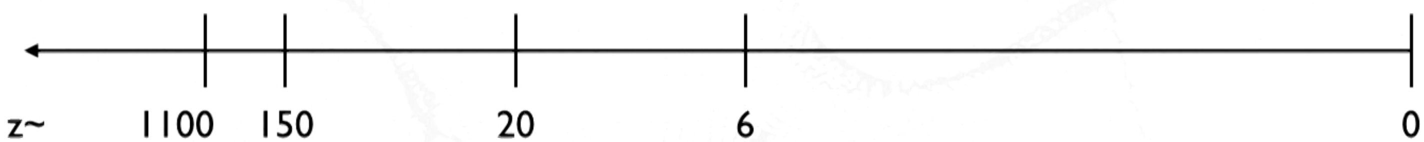

21cm cosmology

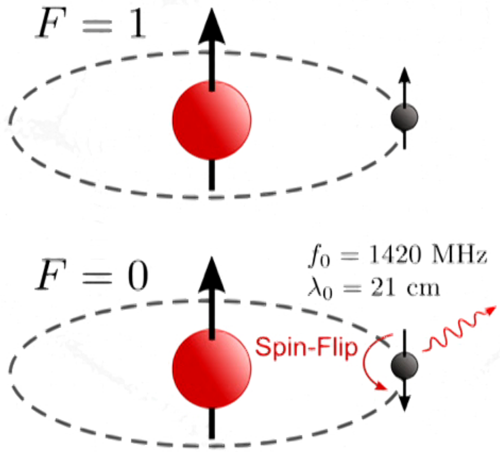

We can use this to map the distribution of neutral hydrogen

$$\lambda_{\rm obs}(z) = \lambda_0(1+z)$$

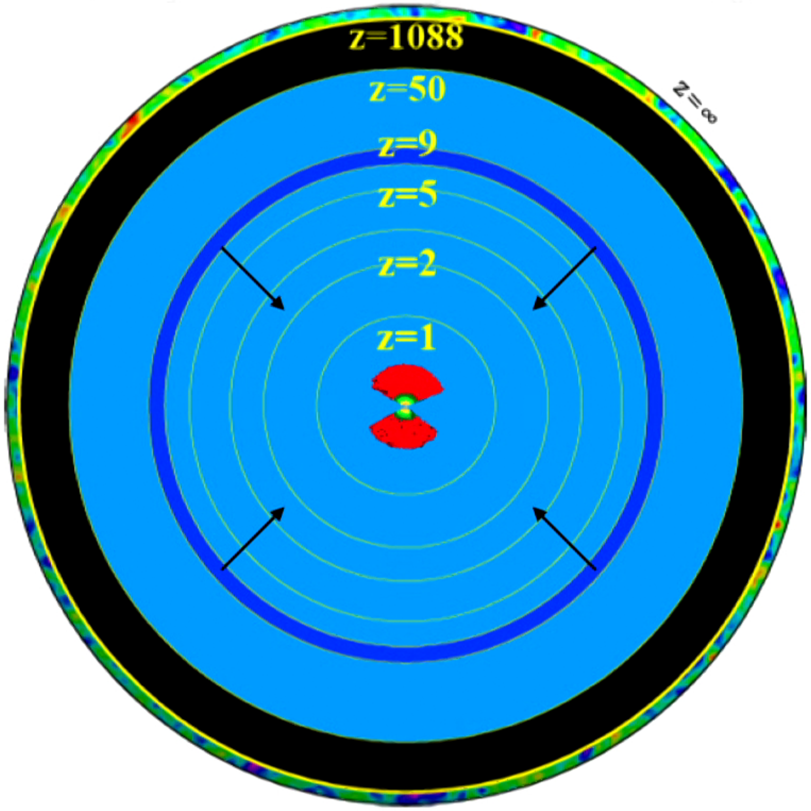

Tegmark et al, 2009

21cm cosmology

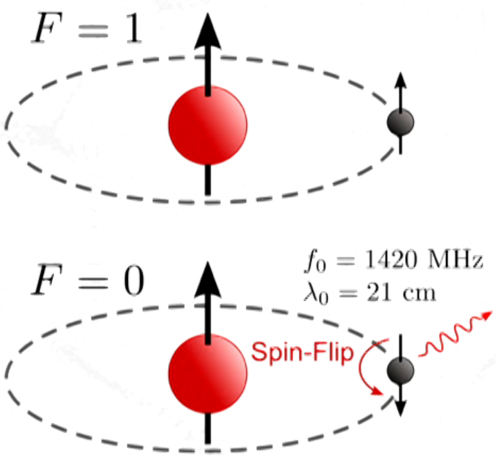

We can use this to map the distribution of neutral hydrogen

$$\lambda_{\rm obs}(z) = \lambda_0(1+z)$$

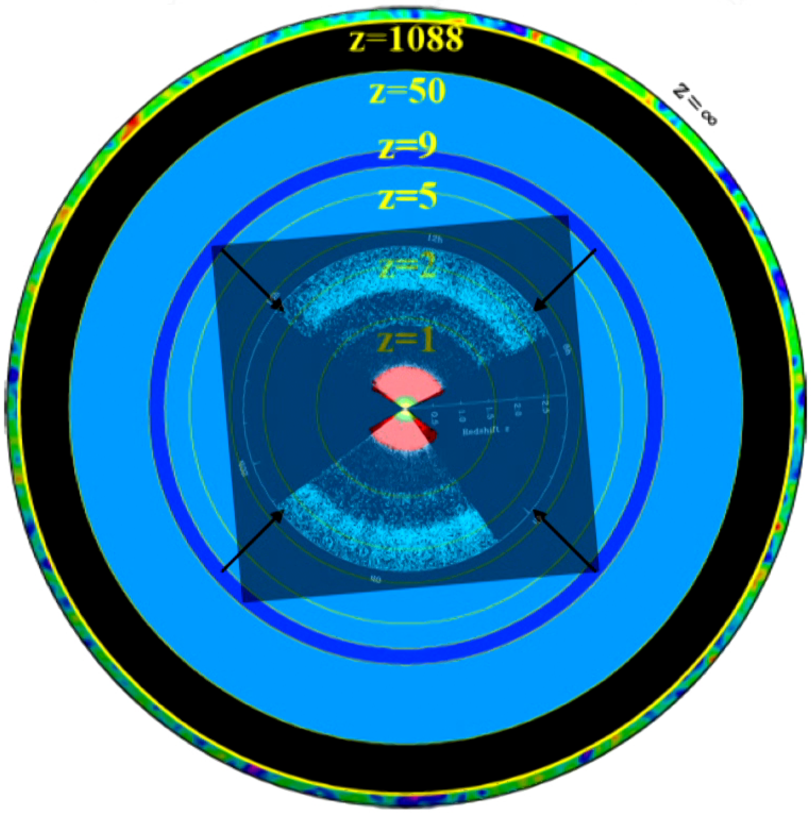

Tegmark et al, 2009

21-cm Cosmology

- Promising probe of LSS
- Intensity mapping (IM) technique
- Foregrounds problem!
- Reionization probes: PAPER, HERA, LOFAR, MWA etc.
- We will focus on low-z where HI resides in galaxies
- Many probes are targeting the BAO peak at z<3: SKA, CHIME, HIRAX, Tianlai, FAST, BINGO, BAOBAB etc.
- Two approaches: single dish & interferometers

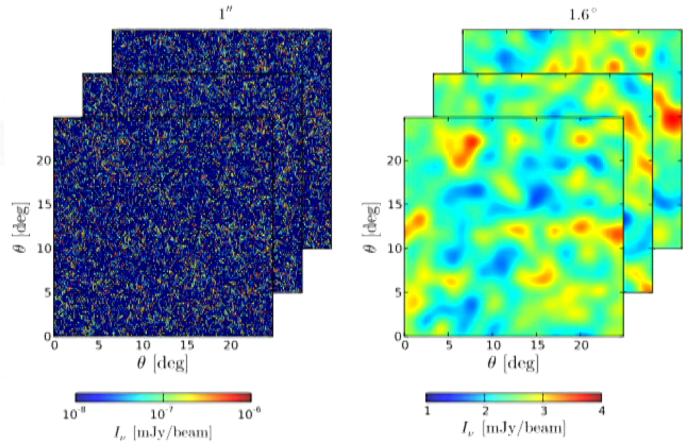

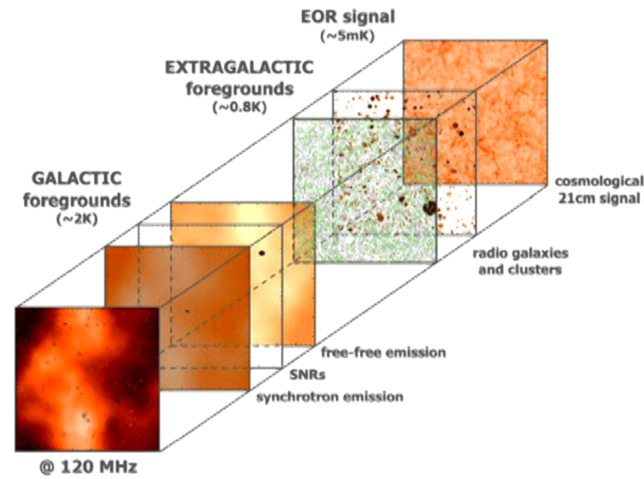

Foregrounds

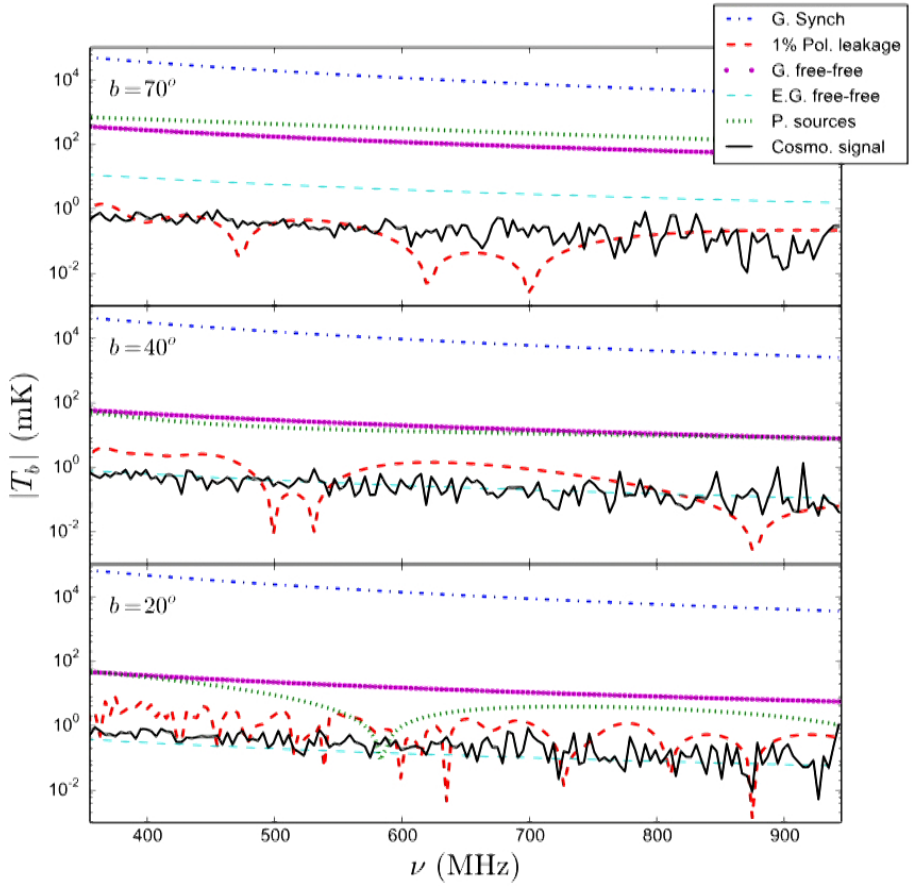

Alonso et al, 2014

Power spectrum of HI

At the linear level:

$$P_{21}(k,z,\mu) = \overline{T}_{\rm b}^2(z)\left(b_{\rm HI}(z) + f(z)\mu^2\right)^2 P_{\rm m}(k,z)$$

$$\overline{T}_{\rm b}(z) = 180\frac{H_0(1+z)^2}{H(z)}\Omega_{\rm HI}(z) h \mathrm{mK}$$

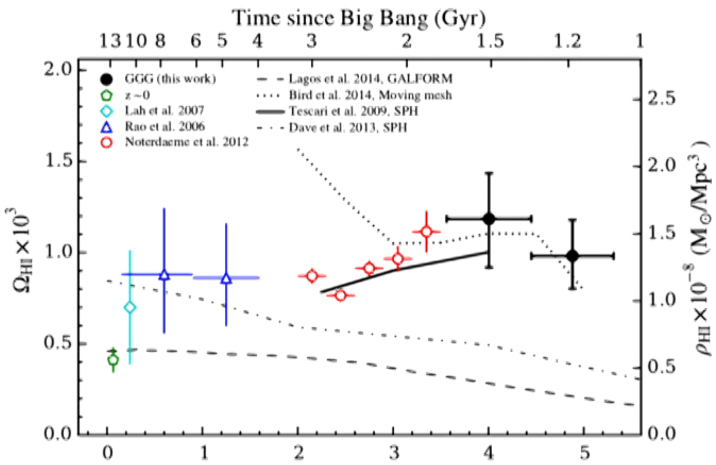

Crighton+15, Bird+16

Power spectrum of HI

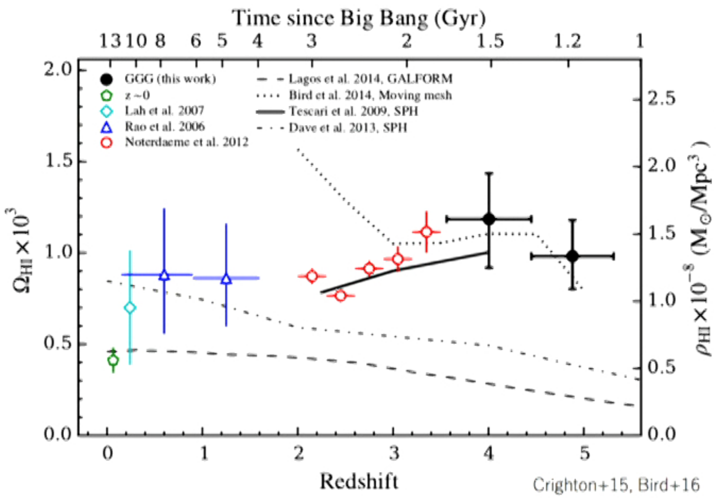

Crighton+15, Bird+16

At the linear level:

$$P_{21}(k,z,\mu) = \overline{T}_{\rm b}^2(z)\left(b_{\rm HI}(z) + f(z)\mu^2\right)^2 P_{\rm m}(k,z)$$

$$\overline{T}_{\rm b}(z) = 180\frac{H_0(1+z)^2}{H(z)}\Omega_{\rm HI}(z) h \rm mK$$

Using the halo model:

$$P_{21,\rm 1h}(k) \equiv \int_0^\infty n(M_h)\left[\frac{M_{\rm HI}(M_h)}{\bar{\rho}_{\rm HI}} u_{\rm HI}(k|M_h)\right]^2 dM_h$$

$$P_{21,\rm 2h}(k) \equiv P_{\rm m}(k)\left[\int_0^\infty n(M_h)\, b(M_h)\left[\frac{M_{\rm HI}(M_h)}{\bar{\rho}_{\rm HI}} u_{\rm HI}(k|M_h)\right] dM_h\right]^2$$

$$P_{21} = P_{21,\rm 1h} + P_{21,\rm 2h}$$

Two ingredients necessary:

Power spectrum of HI

At the linear level:

$$P_{21}(k,z,\mu) = \overline{T}_{\rm b}^2(z)\left(b_{\rm HI}(z) + f(z)\mu^2\right)^2 P_{\rm m}(k,z)$$

$$\overline{T}_{\rm b}(z) = 180\frac{H_0(1+z)^2}{H(z)}\Omega_{\rm HI}(z)h{\rm mK}$$

Using the halo model:

$$P_{21,{\rm 1h}}(k) \equiv \int_0^\infty n\left(M_h\right)\left[\frac{M_{\rm HI}\left(M_h\right)}{\bar{\rho}_{\rm HI}}u_{\rm HI}(k|M_h)\right]^2 dM_h$$

$$P_{21,{\rm 2h}}(k) \equiv P_{\rm m}(k)\left[\int_0^\infty n\left(M_h\right)b(M_h)\left[\frac{M_{\rm HI}\left(M_h\right)}{\bar{\rho}_{\rm HI}}u_{\rm HI}(k|M_h)\right]dM_h\right]^2$$

$$P_{21} = P_{21,{\rm 1h}} + P_{21,{\rm 2h}}$$

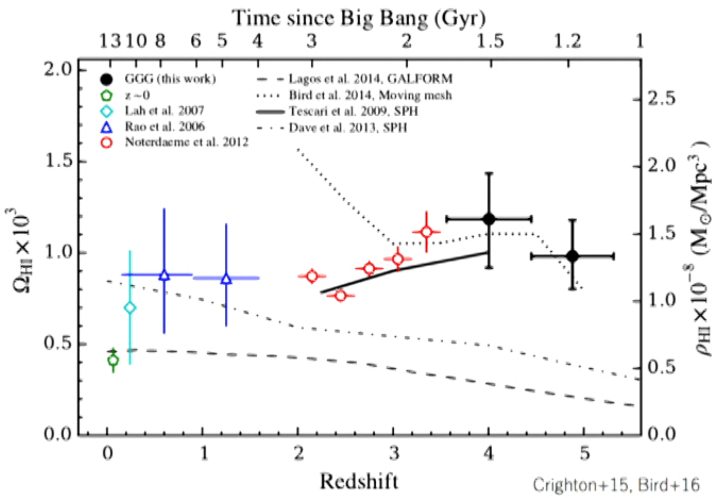

Two ingredients necessary:

$$M_{\rm HI}\left(M_h\right) = M_0\left(\frac{M_h}{M_{\rm min}}\right)^\alpha \exp\left(-\frac{M_{\rm min}}{M_h}\right)$$

$$u_{\rm HI}(k|M) = \frac{4\pi}{M_{\rm HI}(M_h)}\int_0^{R_{\rm v}}\rho_{\rm HI}(r)\frac{\sin kr}{kr}r^2{\rm d}r$$

$$\Omega_{\rm HI} = \frac{1}{\rho_{\rm c}}\int_0^\infty dM_h n\left(M_h\right)M_{\rm HI}\left(M_h\right)$$

$$b_{\rm HI}(z) = \frac{\int_0^\infty b\left(M_h,z\right)n\left(M_h,z\right)M_{\rm HI}\left(M_h,z\right)dM_h}{\int_0^\infty n\left(M_h,z\right)M_{\rm HI}\left(M_h,z\right)dM_h}$$

Power spectrum of HI

At the linear level:

$$P_{21}(k,z,\mu) = \overline{T}_{\rm b}^2(z)\left(b_{\rm HI}(z) + f(z)\mu^2\right)^2 P_{\rm m}(k,z)$$

$$\overline{T}_{\rm b}(z) = 180\frac{H_0(1+z)^2}{H(z)}\Omega_{\rm HI}(z) h \mathrm{mK}$$

Using the halo model:

$$P_{21,\rm 1h}(k) \equiv \int_0^\infty n(M_h)\left[\frac{M_{\rm HI}(M_h)}{\bar{\rho}_{\rm HI}} u_{\rm HI}(k|M_h)\right]^2 dM_h$$

$$P_{21,\rm 2h}(k) \equiv P_{\rm m}(k)\left[\int_0^\infty n(M_h)\, b(M_h)\left[\frac{M_{\rm HI}(M_h)}{\bar{\rho}_{\rm HI}} u_{\rm HI}(k|M_h)\right] dM_h\right]^2$$

$$P_{21} = P_{21,\rm 1h} + P_{21,\rm 2h}$$

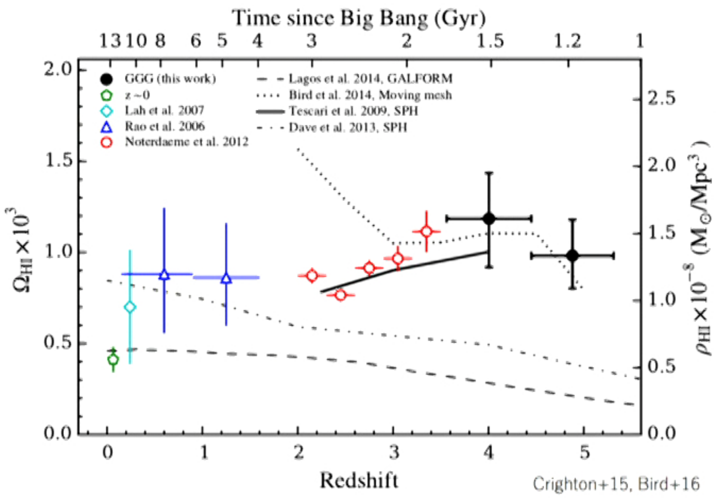

Crighton+15, Bird+16

Two ingredients necessary:

$$M_{\rm HI}(M_h) = M_0\left(\frac{M_h}{M_{\rm min}}\right)^\alpha \exp\left(-\frac{M_{\rm min}}{M_h}\right)$$

$$\Omega_{\rm HI} = \frac{1}{\rho_c}\int_0^\infty dM_h n(M_h) M_{\rm HI}(M_h)$$

$$b_{\rm HI}(z) = \frac{\int_0^\infty b(M_h,z)\, n(M_h,z)\, M_{\rm HI}(M_h,z)\, dM_h}{\int_0^\infty n(M_h,z)\, M_{\rm HI}(M_h,z)\, dM_h}$$

$$u_{\rm HI}(k|M) = \frac{4\pi}{M_{\rm HI}(M_h)}\int_0^{R_v} \rho_{\rm HI}(r)\frac{\sin kr}{kr} r^2 \mathrm{d}r$$

$$\rho_{\rm HI}(r|M_h) \propto (r + 3/4r_s)^{-1}(r+r_s)^{-2}$$

$$\rho_{\rm HI}(r|M_h) \propto \exp(-r/r_s)$$

Questions we try to answer

- How to perform BAO reconstruction with 21cm IM using single dish antenna?
- What could we learn about the growth, BAO, neutrino masses etc. using 21cm IM studies in the redshift range $2.5<z<5$?
- What is the HI content of dark matter haloes at $z \approx 0$ from real data (ALFALFA & SDSS)? What is the HI bias at $z \approx 0$?

21cm Intensity Mapping with single dish

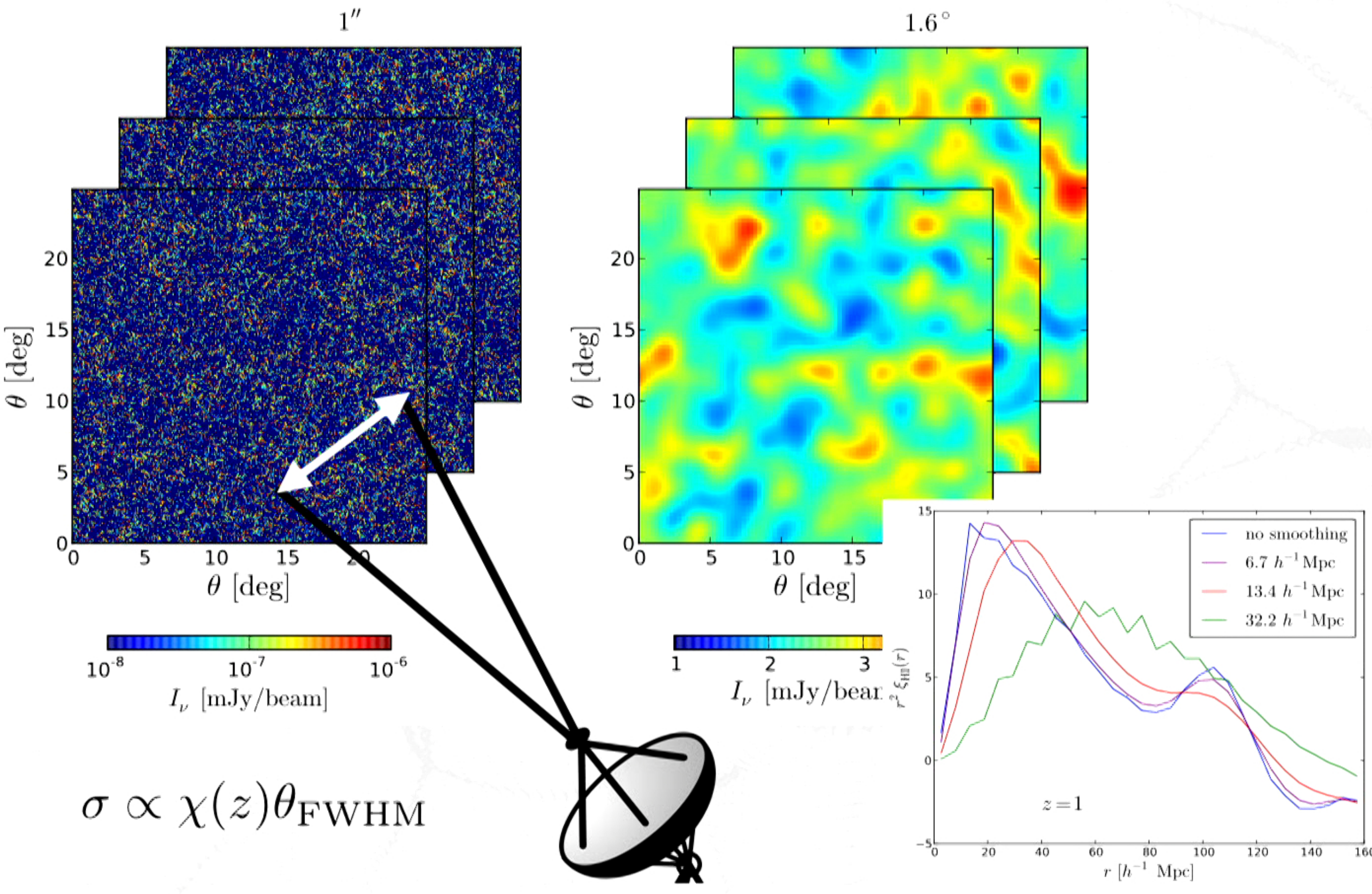

$$\sigma \propto \chi(z)\theta_{\mathrm{FWHM}}$$

Effect of 2D smoothing in linear theory

2D smoothing introduces anisotropy in the power spectrum

$$P_{2D}(k,\mu) = P(k)e^{-k^2(1-\mu^2)\sigma^2} \qquad P_{2D}(k,\mu) = (1+\beta\mu^2)^2 P(k)e^{-k^2(1-\mu^2)\sigma^2}$$

We continue the analysis using Legendre multipoles:

$$P_{l,t}(k) = \frac{2l+1}{2}\int_{-1}^{1} P_t(k,\mu)L_l(\mu)d\mu \longleftrightarrow \xi_{l,t}(r) = i^l \int \frac{k^3 d\log(k)}{2\pi^2} P_{l,t}(k)j_l(kr)$$

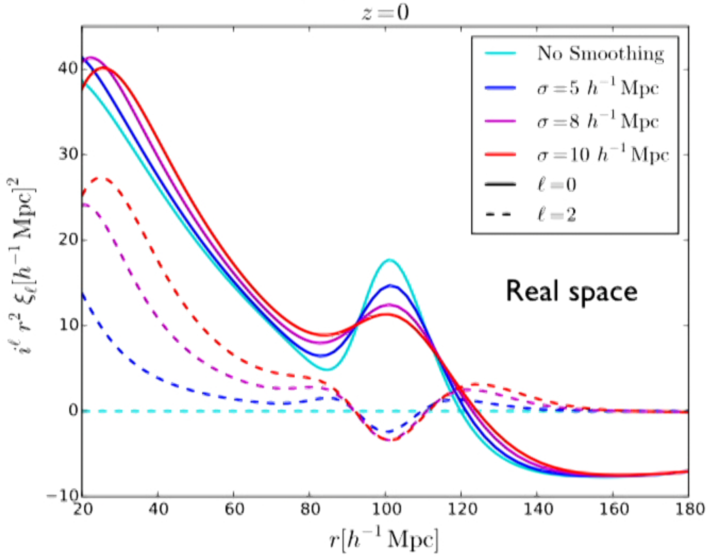

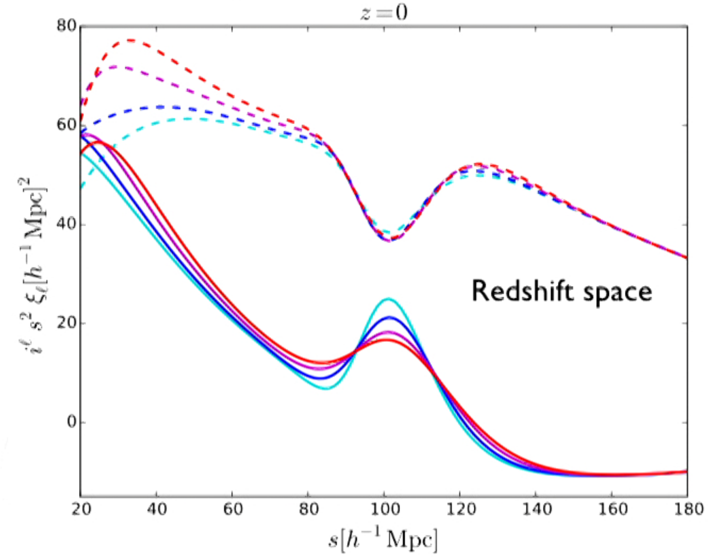

Standard reconstruction algorithm

- Smooth the density field $\delta(\vec{k}) \rightarrow S(\vec{k})\delta(\vec{k}) \quad S(\vec{k}) = e^{-(kR_\Psi)^2/2}$
- Compute negative Zel'dovich displacement field on a grid $$\vec{s}(\vec{k}) \equiv -i\frac{\vec{k}}{k^2}S(\vec{k})\delta(\vec{k})$$
- Displace original particles by s - "displaced" $$\delta_d(\vec{k}) = \int d^3q e^{-i\vec{k}\cdot\vec{q}}(e^{-i\vec{k}\cdot\left(\vec{\Psi}(\vec{q})+\vec{s}(\vec{q})\right)} - 1)$$
- Shift spatially uniform grid of particles - "shifted" $$\delta_s(\vec{k}) = \int d^3q e^{-i\vec{k}\cdot\vec{q}}(e^{-i\vec{k}\cdot\vec{s}(\vec{q})} - 1)$$
- Reconstructed density field $$\delta_{recon} \equiv \delta_d - \delta_s$$

Padmanabhan et al, 2009

Standard BAO reconstruction

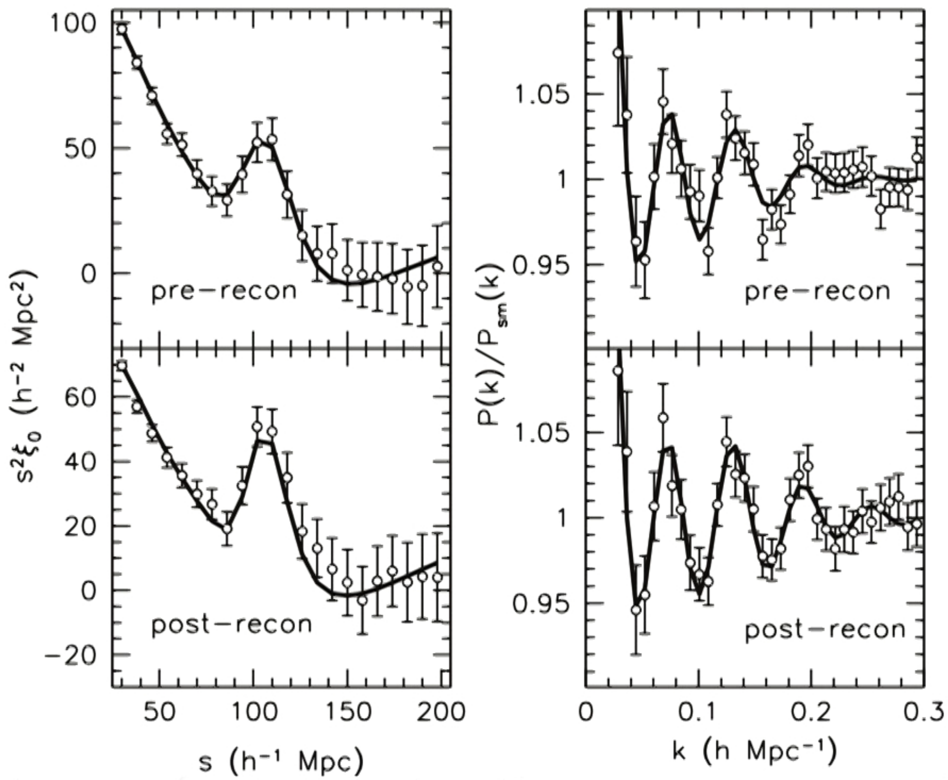

BOSS DR11

Anderson et al, 2014

How to reconstruct 2D smoothed maps?

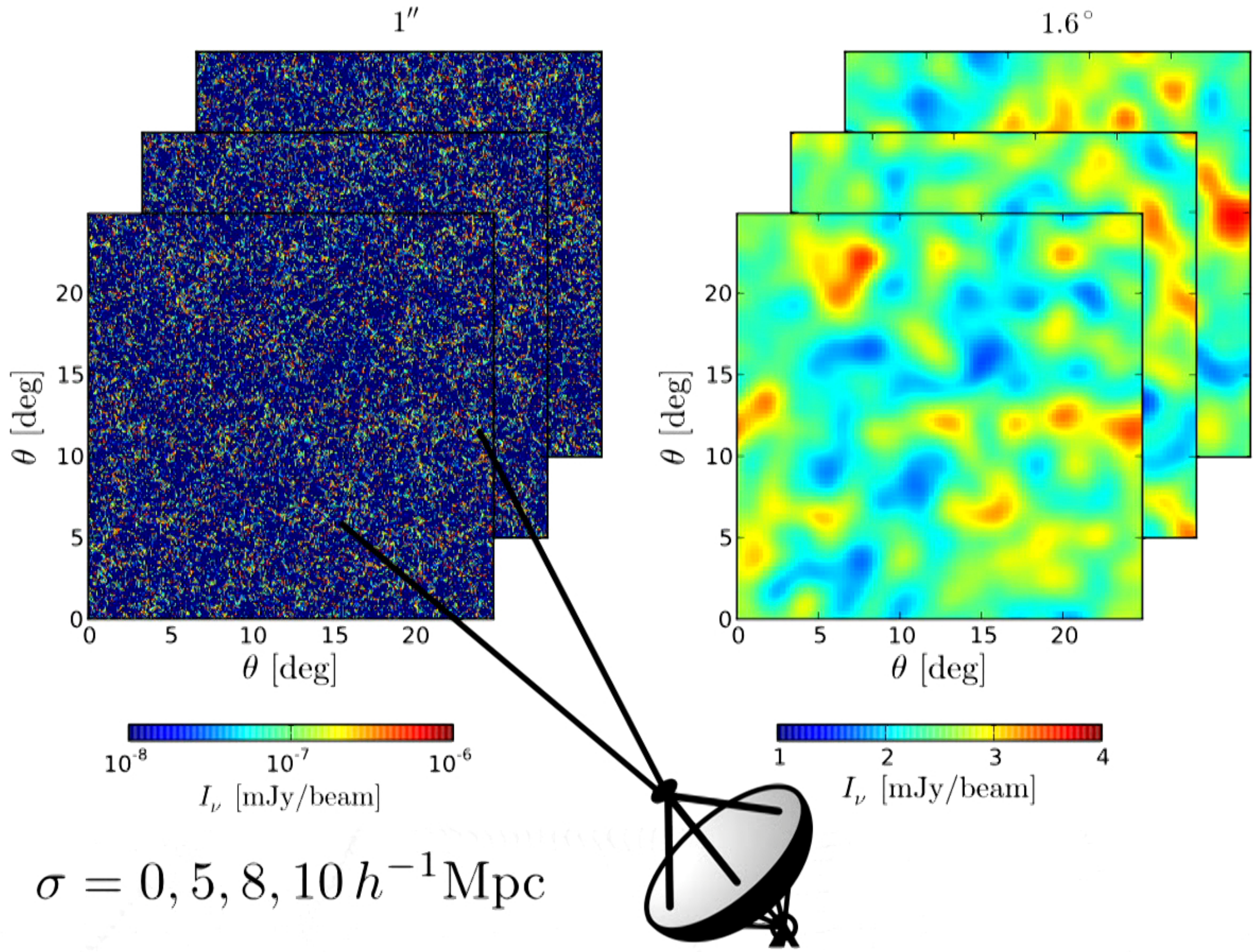

$$\sigma = 0, 5, 8, 10\, h^{-1}\mathrm{Mpc}$$

How to reconstruct 2D smoothed maps?

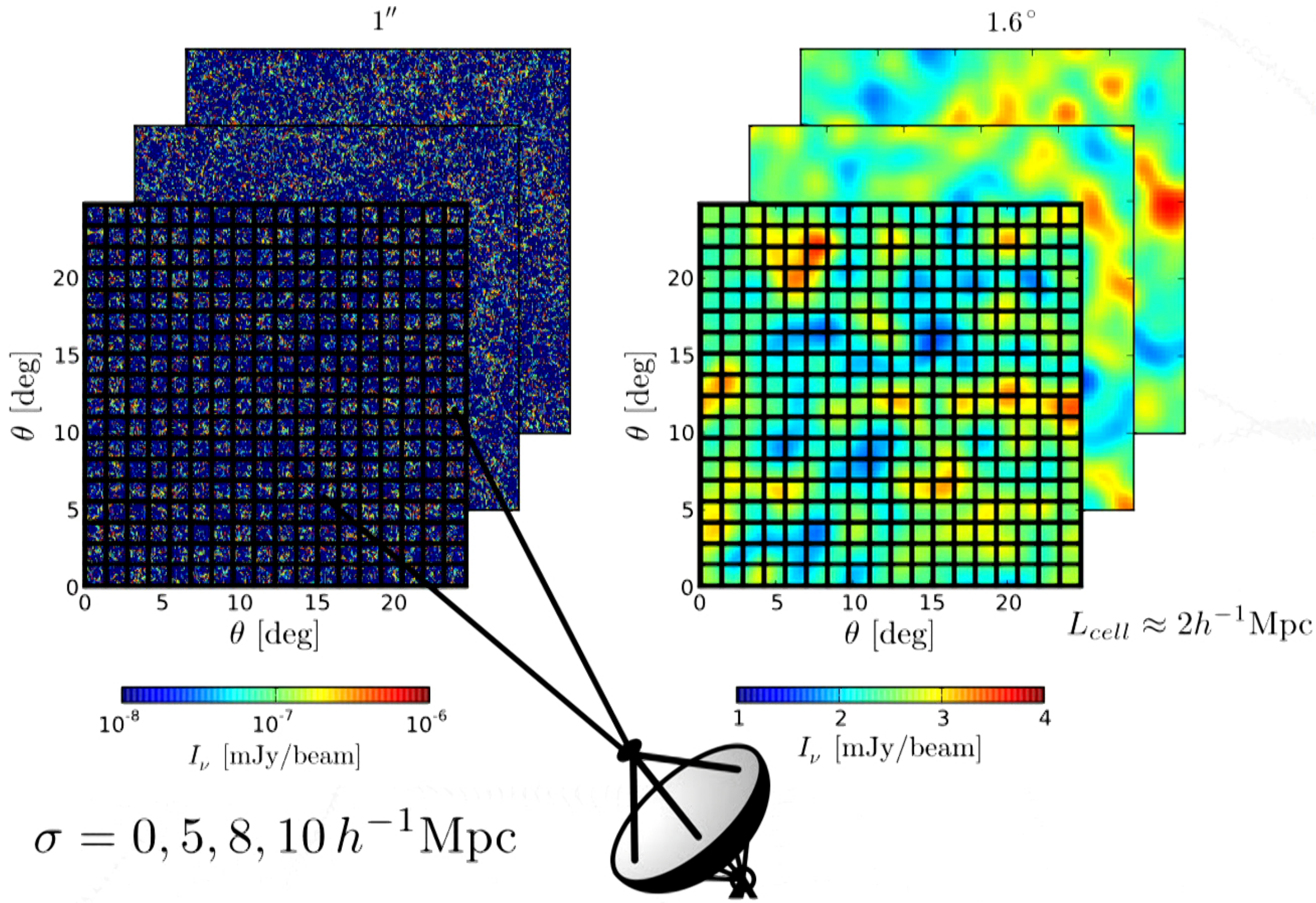

$$\sigma = 0, 5, 8, 10\, h^{-1}\mathrm{Mpc}$$

Reconstruction algorithm

- Smooth the density field $$\delta(\vec{k}) \rightarrow S(\vec{k})\delta(\vec{k})$$
- Compute negative Zel'dovich displacement field on a grid $$\vec{s}(\vec{k}) \equiv -i\frac{\vec{k}}{k^2}S(\vec{k})\delta(\vec{k})$$
- Displace ~~original particles~~ grid cells by s - "displaced" $$\delta_d(\vec{k}) = \int d^3q e^{-i\vec{k}\cdot\vec{q}}(e^{-i\vec{k}\cdot\left(\vec{\Psi}(\vec{q})+\vec{s}(\vec{q})\right)} - 1)$$
- ~~Shift spatially uniform grid of particles - "shifted"~~ apply uniform weights to displaced grid positions $$\delta_s(\vec{k}) = \int d^3q e^{-i\vec{k}\cdot\vec{q}}(e^{-i\vec{k}\cdot\vec{s}(\vec{q})} - 1)$$
- Reconstructed density field $$\delta_{recon} \equiv \delta_d - \delta_s$$

N-body simulations

- We ran 500 L-PICOLA simulations (Howlett et al, 2015)
- BoxSize — 1 Gpc/h
- Number of particles 512^3, number of timesteps to z=0 — 50
- We simulate the intrinsic resolution of 21cm maps by applying a 2D Gaussian filter to the overdensity field: $\tilde{\delta}_{\rm sm}(\mathbf{k}) = \tilde{\delta}(\mathbf{k}) e^{-k^2(1-\mu^2)\sigma^2/2}$
- We call these mock maps: matter and halo maps
- The case of no angular smoothing corresponds to "galaxy" survey

Initial vs reconstructed field

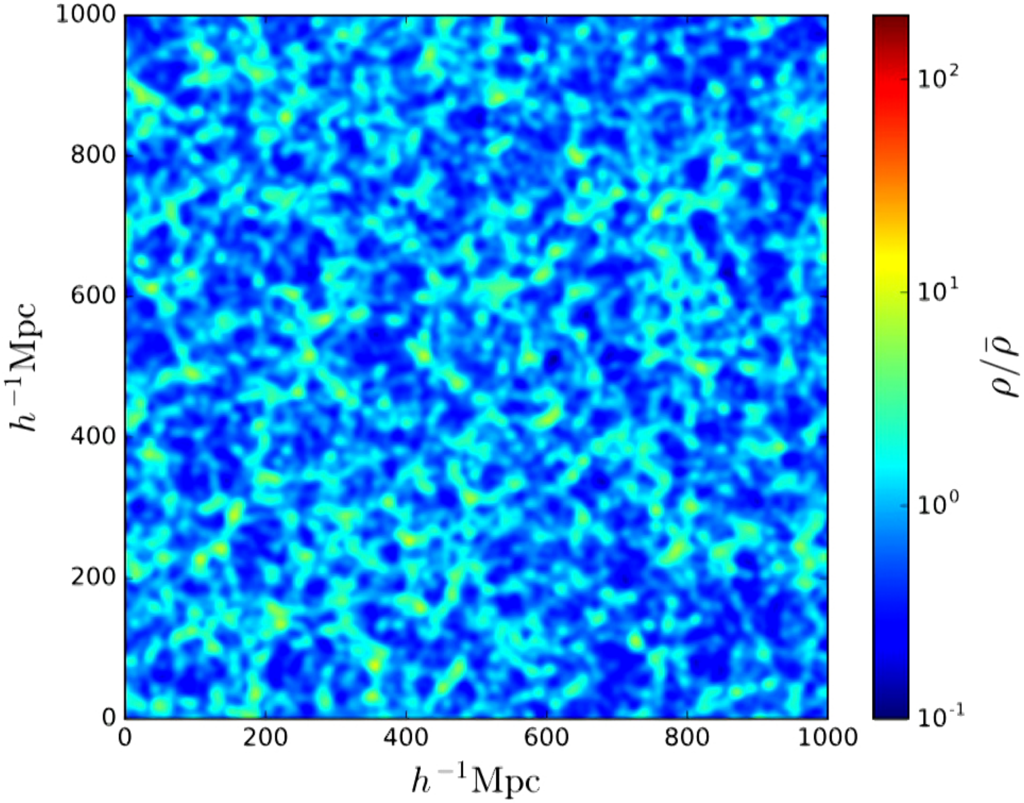

Comparison for a "galaxy survey"

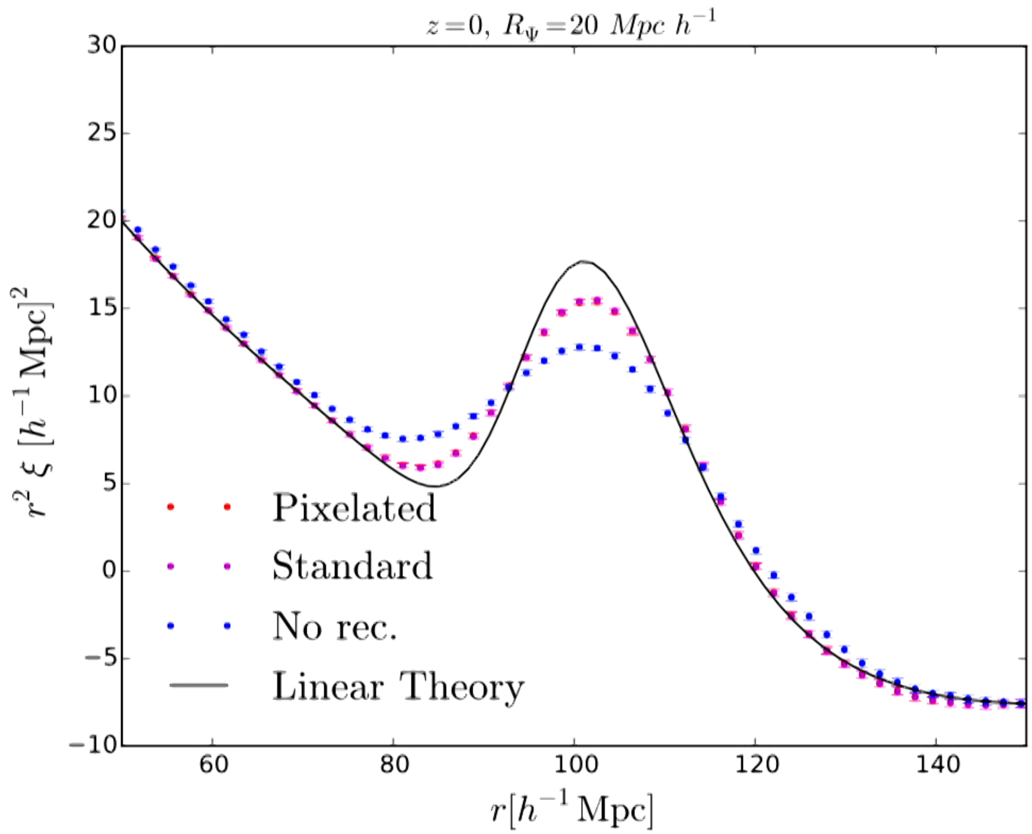

Matter maps

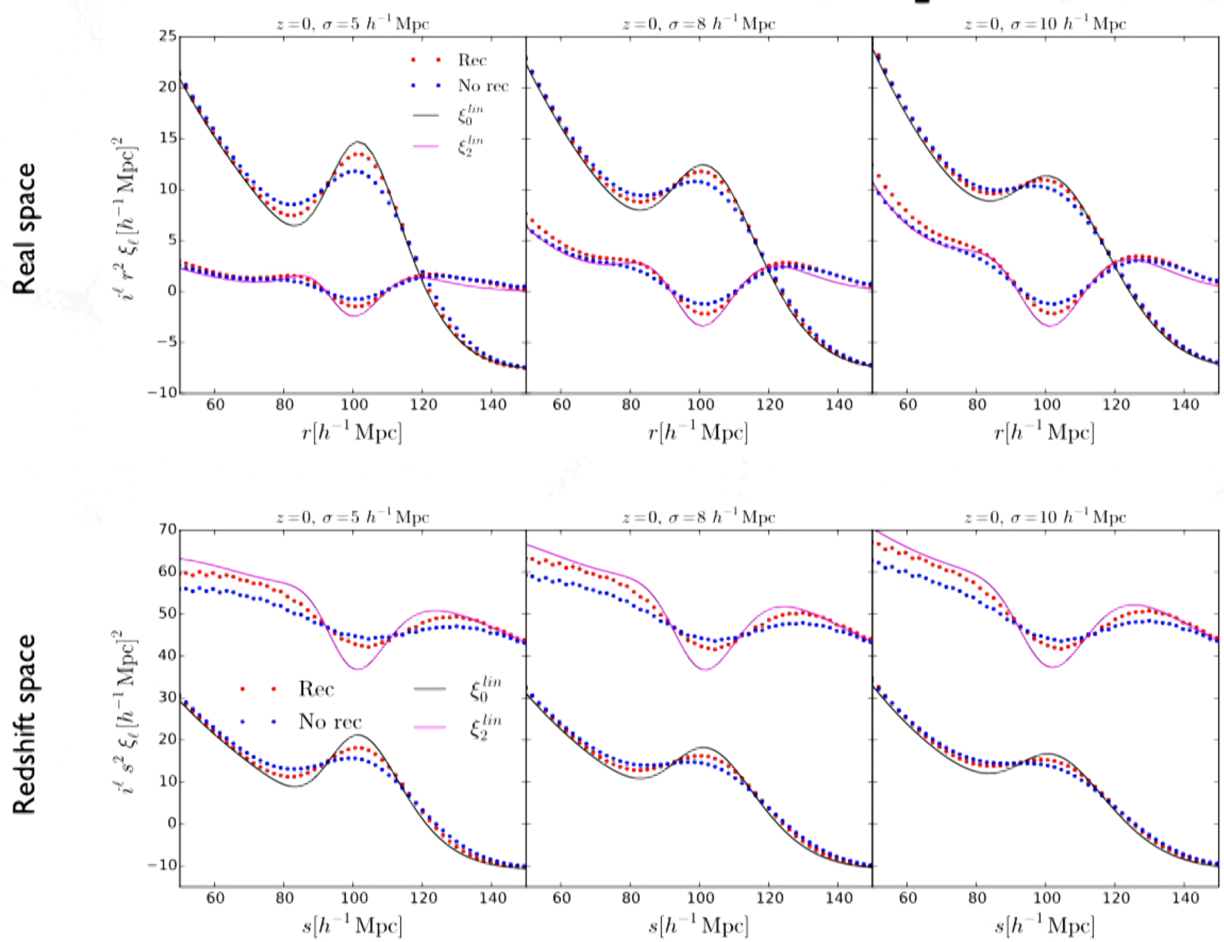

Real space
Redshift space
$z=0,\ \sigma=5\ h^{-1}$Mpc
$z=0,\ \sigma=8\ h^{-1}$Mpc
$z=0,\ \sigma=10\ h^{-1}$Mpc
Rec
No rec
ξ_0^{lin}
ξ_2^{lin}
$i^\ell\, r^2\, \xi_\ell\, [h^{-1}\,\mathrm{Mpc}]^2$
$r[h^{-1}\,\mathrm{Mpc}]$
$i^\ell\, s^2\, \xi_\ell\, [h^{-1}\,\mathrm{Mpc}]^2$
$s[h^{-1}\,\mathrm{Mpc}]$

Halo maps

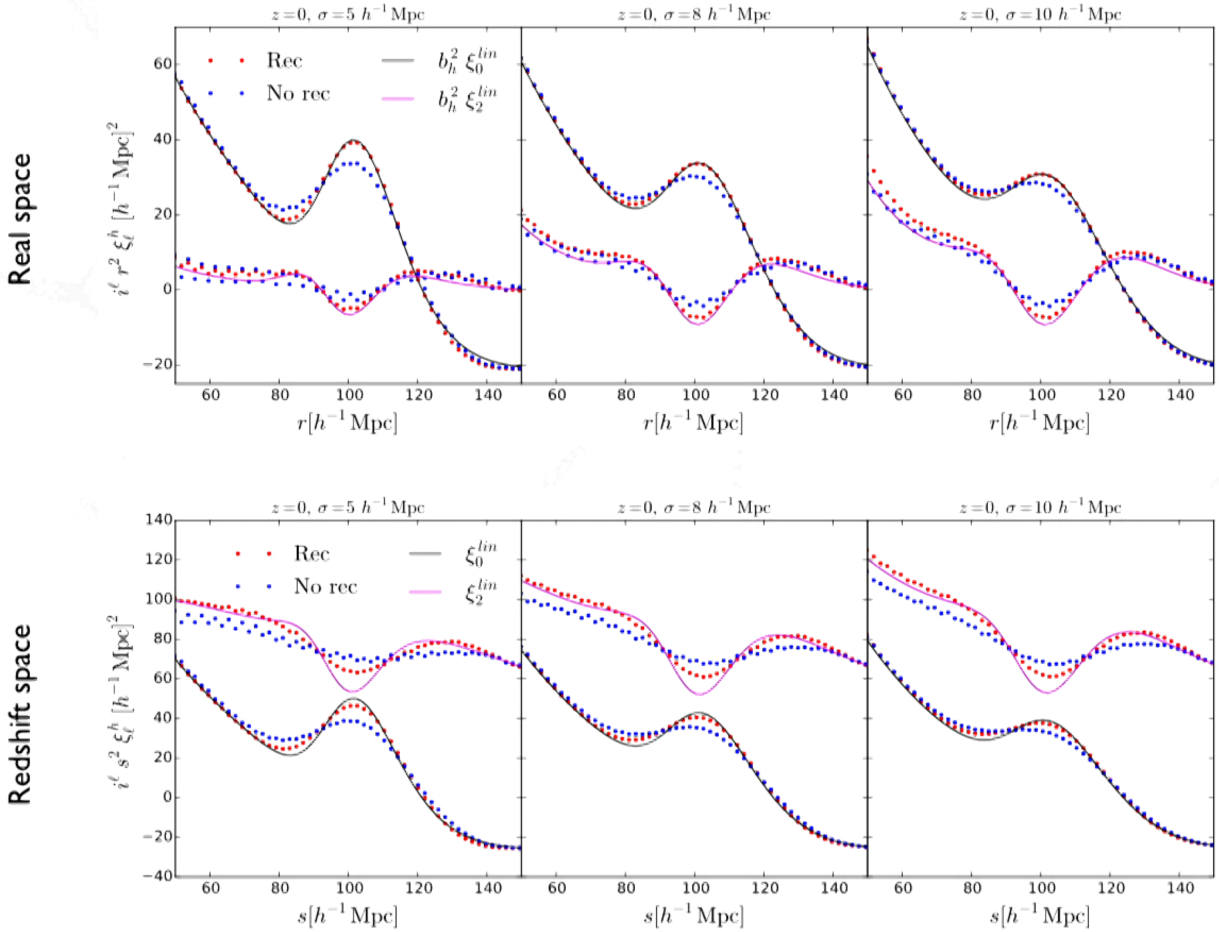

Real space
Redshift space
$z=0,\ \sigma=5\ h^{-1}\mathrm{Mpc}$
$z=0,\ \sigma=8\ h^{-1}\mathrm{Mpc}$
$z=0,\ \sigma=10\ h^{-1}\mathrm{Mpc}$
Rec
No rec
$b_h^2\ \xi_0^{lin}$
$b_h^2\ \xi_2^{lin}$
ξ_0^{lin}
ξ_2^{lin}
$i^\ell\ r^2\ \xi_\ell^h\ [h^{-1}\mathrm{Mpc}]^2$
$i^\ell\ s^2\ \xi_\ell^h\ [h^{-1}\mathrm{Mpc}]^2$
$r[h^{-1}\mathrm{Mpc}]$
$s[h^{-1}\mathrm{Mpc}]$

What about the BAO peak position?

Isotropic shift

$$\alpha = \left[\frac{D_A^2(z)}{D_{A,f}^2(z)} \frac{H_f(z)}{H(z)} \right]^{1/3} \frac{r_{s,f}}{r_s}$$

Anisotropic shift

$$1 + \epsilon = \left[\frac{H_f(z)}{H(z)} \frac{D_{A,f}(z)}{D_A(z)} \right]^{1/3}$$

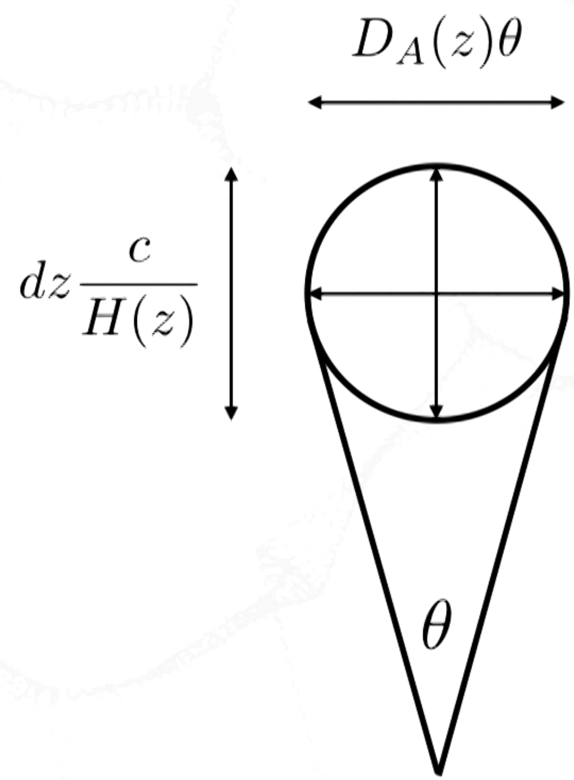

Constraints on the peak position: matter maps in real space

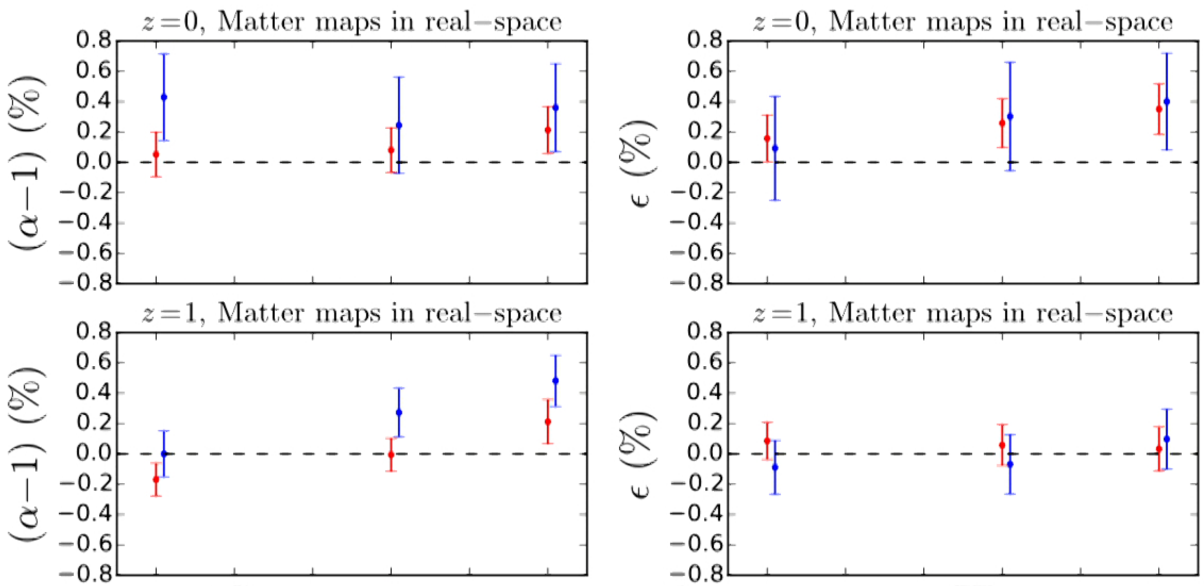

Non Reconstructed
Reconstructed

Main conclusions

- We have tested a modified reconstruction method intended for extracting BAO from future 21cm IM surveys
- We find this method is able to decrease the uncertainty in the BAO peak position by 30-50% over the typical angular resolution scales of 21 cm IM experiments
- This method is faster and more general and can also be applied to galaxies and other low angular-resolution observations

High-redshift post-reionization cosmology with 21cm intensity mapping

with E. Castorina, F. Villaescusa-Navarro & M. Viel

arXiv:1709.07893

HI IM at 2.5<z<5

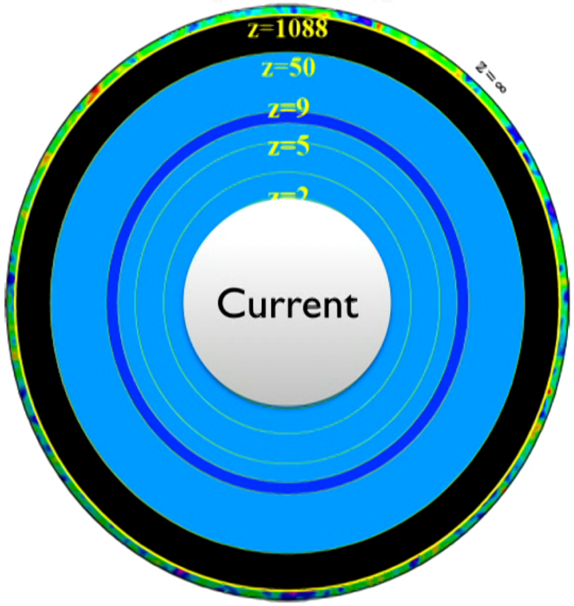

HI IM at 2.5<z<5

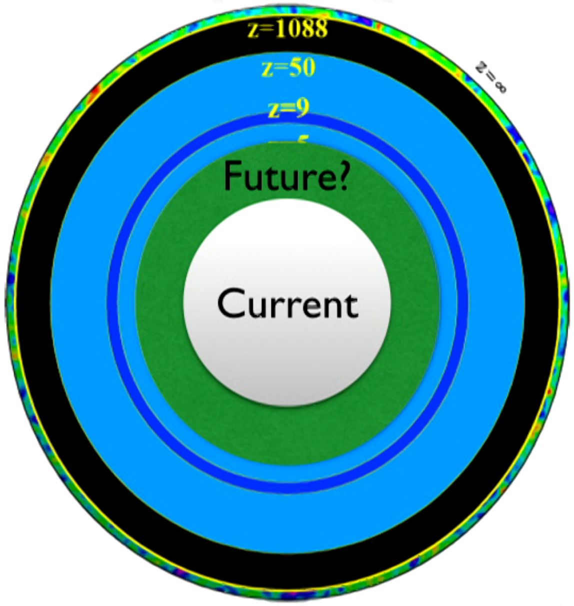

HI IM at 2.5<z<5

- **Advantages**
- More comoving volume: $\frac{V(2.5 < z < 5)}{V(z < 2.5)} \approx 1.4$
- More linear
- Running out of galaxies anyway

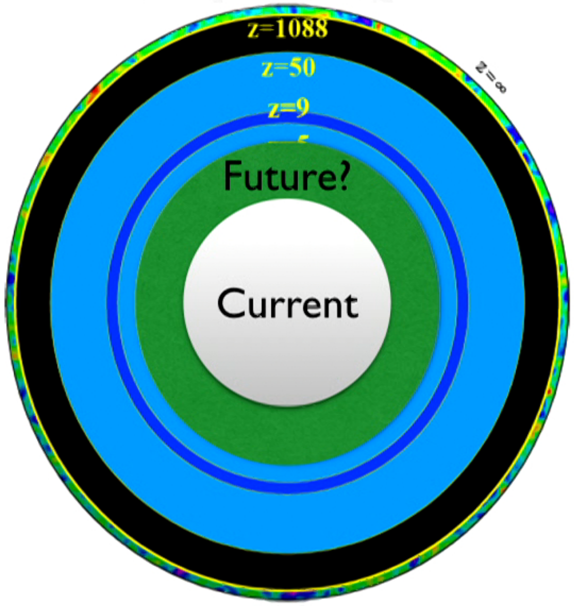

HI IM at 2.5<z<5

- **Advantages**
- More comoving volume: $\frac{V(2.5 < z < 5)}{V(z < 2.5)} \approx 1.4$
- More linear
- Running out of galaxies anyway
- **Disadvantages**
- Foreground problems
- Sky temperature blows up
- Wedge for interferometers
- Angular resolution for single-dish

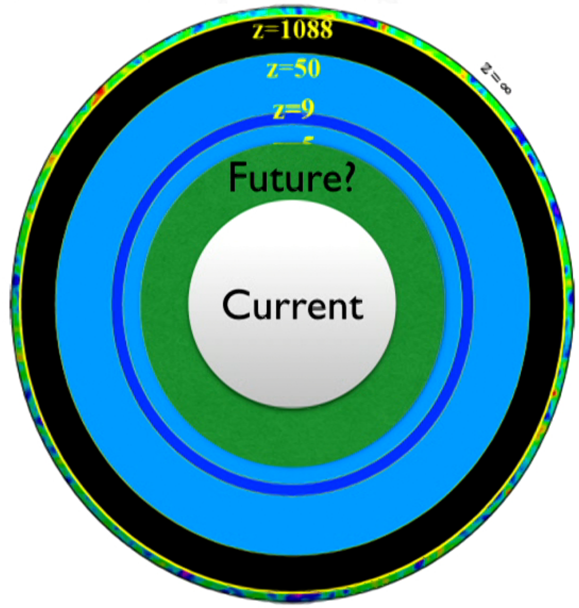

Current experiments

CHIME

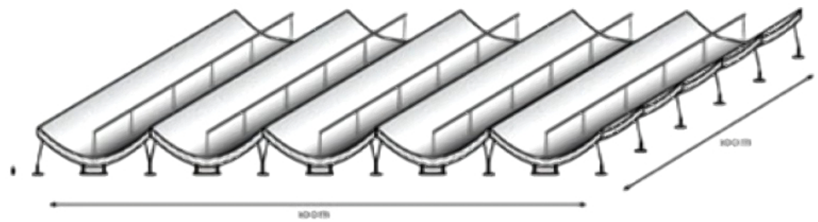

FAST

HIRAX 32x32

Expand current experiments?

2x2xCHIME = Ext-CHIME

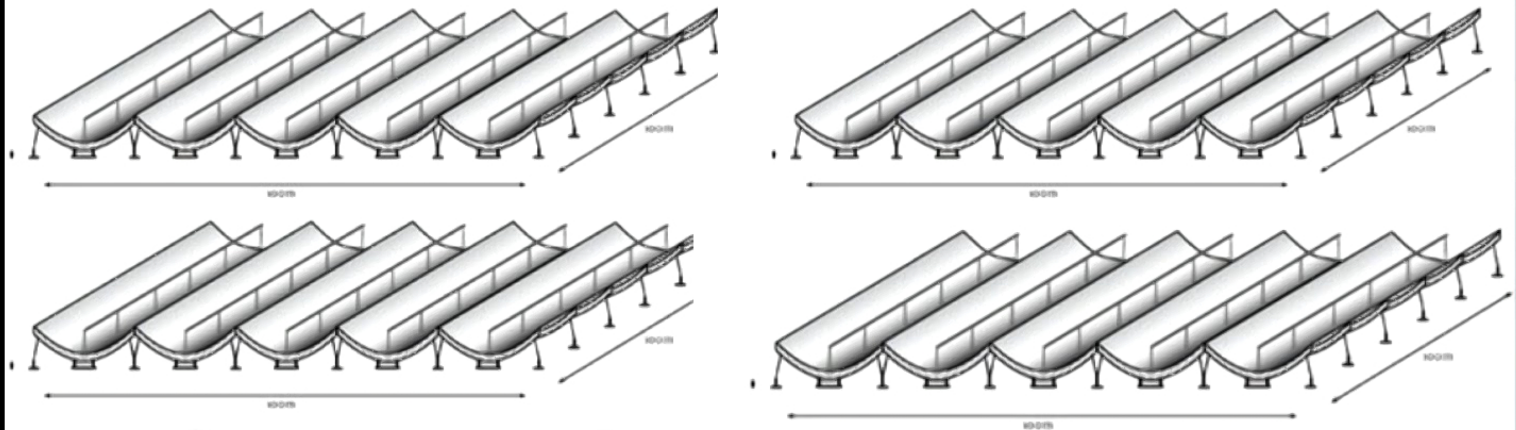

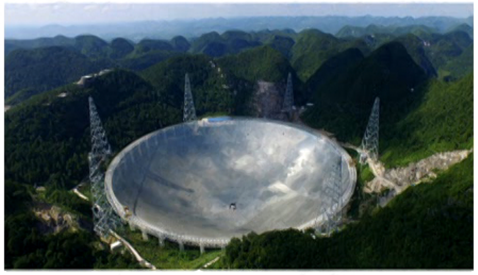

highzFAST

HIRAX 64x64 = Ext-HIRAX

High redshift cosmology with 21cm IM 2.5<z<5.0

We are interested in the following quantities:

- Growth of structures — $f\sigma_8$
- BAO distance-scale parameters — $H(z)\,\&D_A(z)$
- Sum of the neutrino masses — Σm_ν
- Effective number of the neutrino species — $N_{\rm eff}$
- Breaking the degeneracy — $\Sigma m_\nu - w$

Fisher forecasts

Full power spectrum:

$$P_{21}(k_f, \mu_f, z) = \overline{T}_b^2(z) \frac{D_A(z)_f^2 H(z)}{D_A(z)^2 H(z)_f} (b_{\rm HI}\sigma_8(z) + f\sigma_8(z)\mu^2)^2 \frac{P(k,z)}{\sigma_{8,\rm f}^2}$$

Fisher matrix:

$$F_{ij} = \frac{1}{8\pi^2} \int_{-1}^{1} d\mu \int k^2 dk \frac{\partial \ln P_{21}(k,\mu)}{\partial p_i} \frac{\partial \ln P_{21}(k,\mu)}{\partial p_j} V_{\rm eff}(k,\mu)$$

$$V_{\rm eff}(k,\mu) = V_{\rm sur} \left(\frac{P_{21}(k,\mu) W(k,\mu)}{P_{21}(k,\mu) W(k,\mu) + P_{\rm N}^{\rm tot}(k,\mu)} \right)^2$$

Similar to previous forecasts, e.g. Bull et al (2015).
It works under the assumption of Gaussian likelihood and no theoretical uncertainties!
One should be careful about the range of wavenumber considered (kmin, kmax)
We use two different kmax scales — 0.2 & knl(z)=0.2(1+z)^2/3 h/Mpc

Thermal noise

Interferometers

$$P_{\rm N}^{\rm th}(z) = \frac{T_{\rm sys}^2(z)X^2(z)Y(z)\lambda^4(z)S_{21}}{A_{\rm eff}^2{\rm FOV}(z)t_0 n_{\rm pol} n(\mathbf{u},z)}$$

Single-dish

$$P_{\rm N}^{\rm th}(k,\mu) = \frac{T_{\rm sys}^2 V_{\rm pix} W^{-2}(k_\perp)}{\Delta\nu t_{\rm obs}\Omega_{\rm pix}/S_{21} N_{\rm dish} N_{\rm beam}}$$

$$T_{\rm sky}(z) = 60\,{\rm K} \times (\nu_{21}(z)/300{\rm MHz})^{-2.55}$$

Observable modes

Interferometers:

$$k_\perp^{min}(z) = \frac{2\pi D_{min}}{D(z)\lambda(z)}$$

$$k_\perp^{max}(z) = \frac{2\pi D_{max}}{D(z)\lambda(z)}$$

Single-dish:

$$k_\perp^{min}(z) = \frac{2\pi}{\sqrt{D(z)^2 S_{21}}}$$

$$k_\perp^{max}(z) = \frac{2\pi D_{\rm dish}}{D(z)\lambda(z)}$$

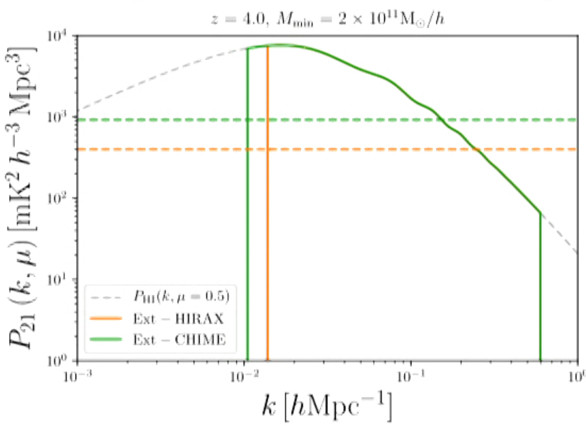

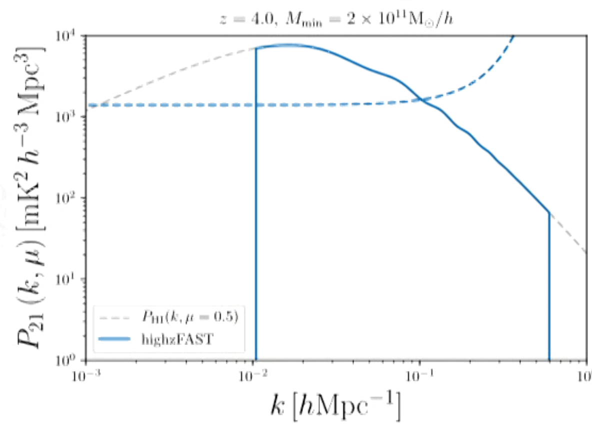

The foreground wedge

Foregrounds are expected to be smooth in frequency,
should affect only low parallel modes,
but the interferometer chromaticity makes them less smooth
as we go to larger baselines, i.e. larger transverse modes.

The wedge:
$$k_{\|} < \sin(\theta_{\rm FoV})\frac{D_c(z)H(z)}{c(1+z)}k_\perp$$

$$\mu_{\rm min}(z) = \frac{k_{\|}}{\sqrt{k_{\|}^2 + k_\perp^2}}$$

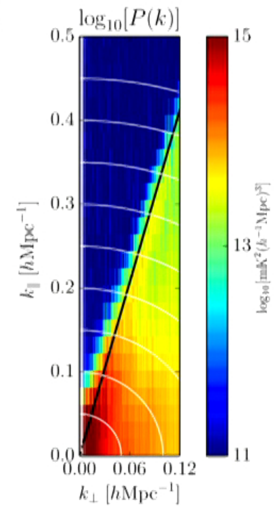

Pober et al, 2015

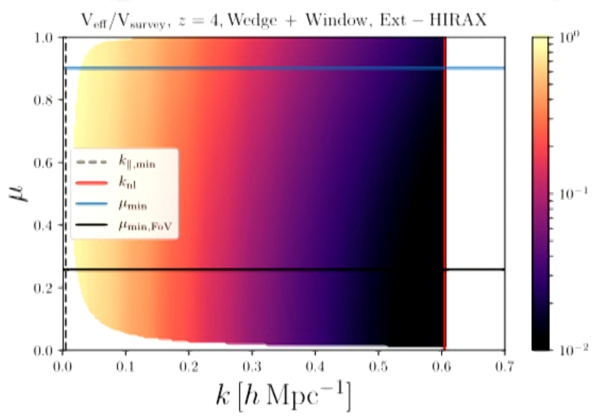

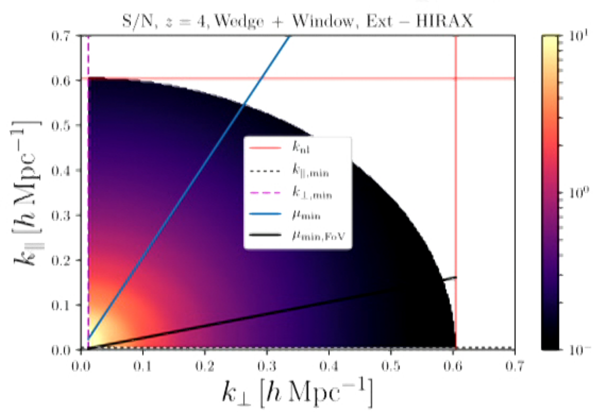

Growth of structures: $f\sigma_8(z)$

2% priors 5% priors

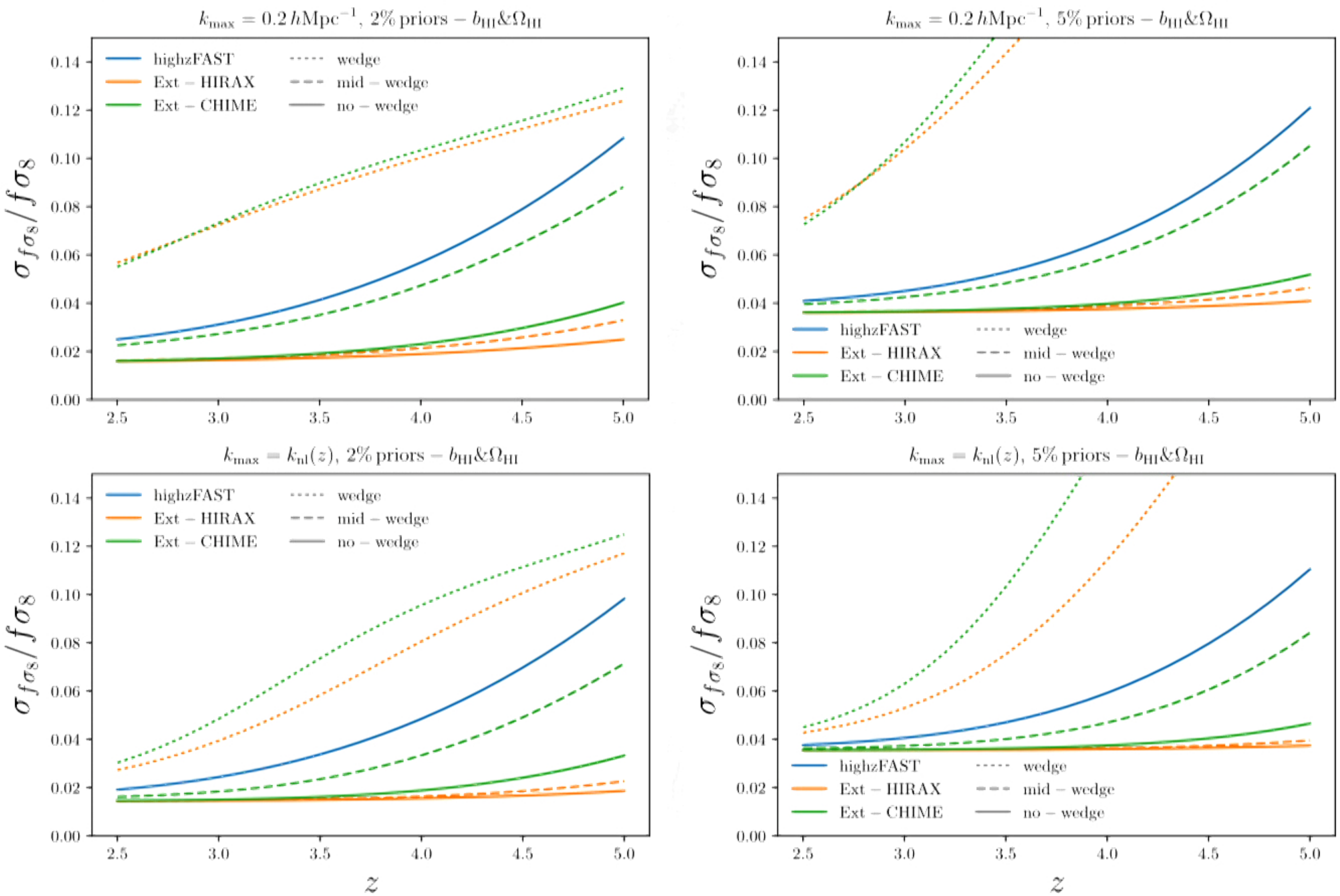

BAO: AP parameters $H(z)$ & $D_A(z)$

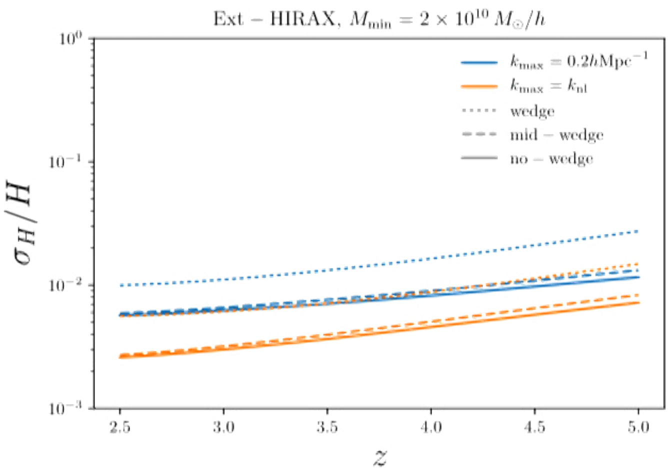

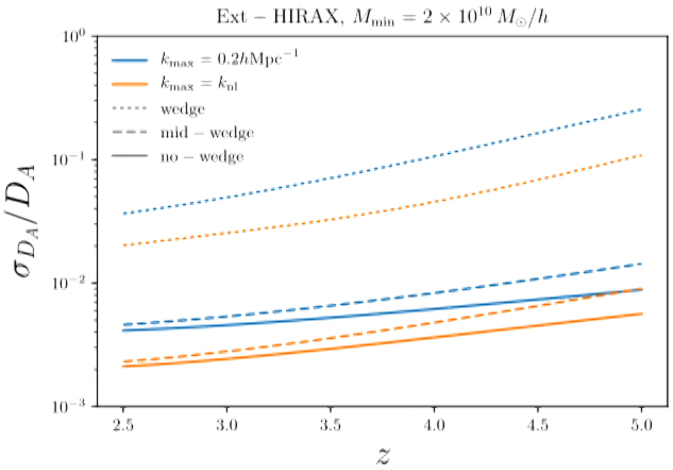

Redshift coverage comparison with other surveys

Growth of structures

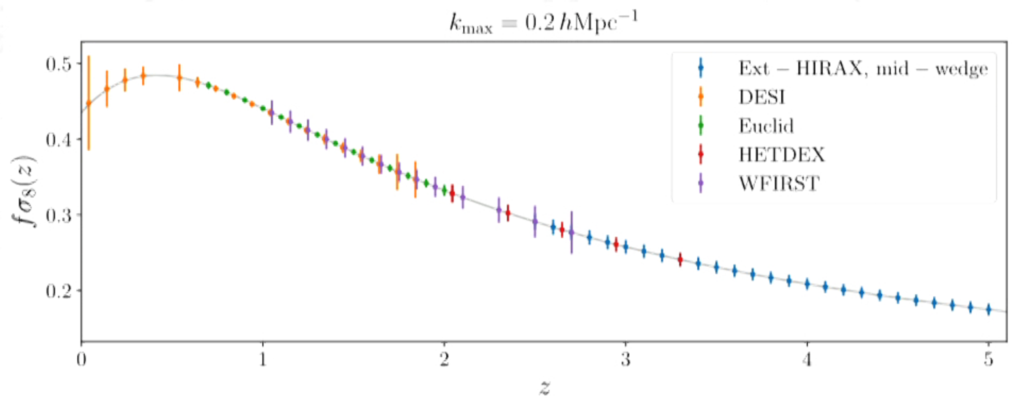

BAO distance scale parameters

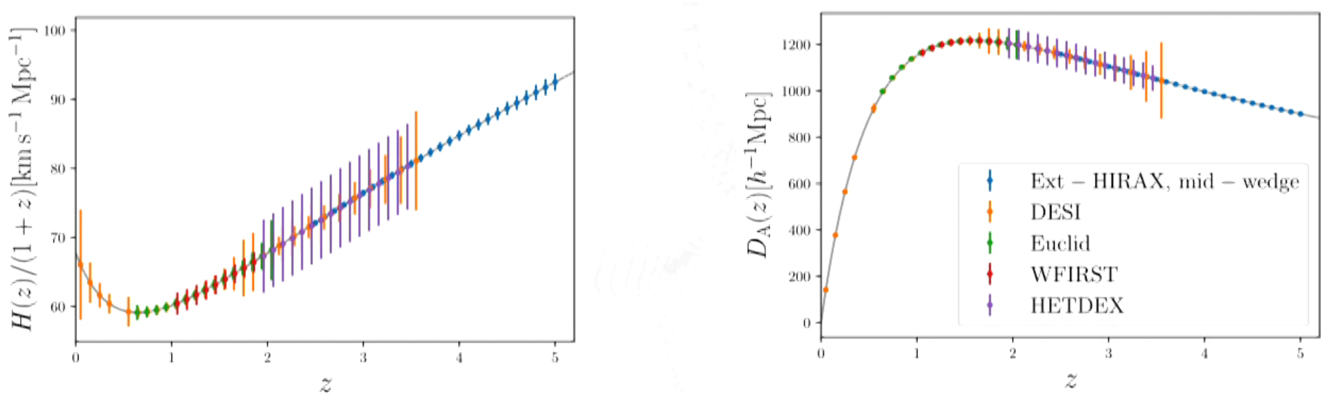

ΛCDM extensions using the broadband shape

- The sum of neutrino masses
- The effective number of relativistic degrees of freedom

We make use of the synergy with current and future datasets and forecasts:

- Planck 2015 + BOSS BAO
- Future galaxy redshift survey — Euclid like
- Future CMB Stage 4 experiment

Broadband shape + massive neutrinos

The effect of massive neutrinos on the power spectrum

CDM+baryons power spectrum

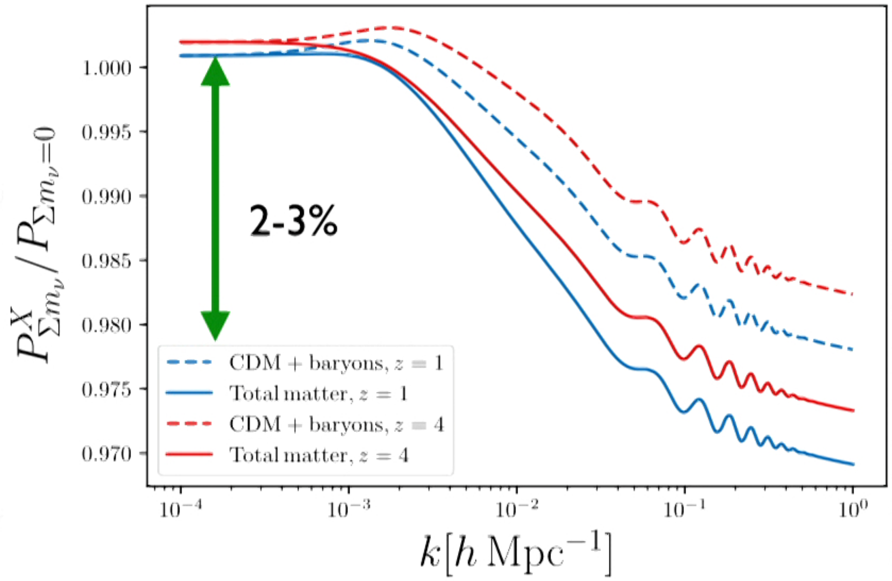

Ext-HIRAX alone

Ext-HIRAX Σm_ν					
	Ω_M	h	Σm_ν[eV]	$\ln(10^{10} A_s)$	n_s
Fiducial values	0.3075	0.6774	0.060	3.064	0.9667
No wedge $k_{max} = 0.2h\mathrm{Mpc}^{-1}$					
2% b_{HI} & Ω_{HI}	0.0016	0.0010	0.059	0.026	0.0036
2% b_{HI} & Ω_{HI}, diff M_{min}	0.0015	0.0009	0.056	0.025	0.0033
2% b_{HI} & Ω_{HI}, 1-loop	0.0020	0.0010	0.081	0.038	0.014
5% b_{HI} & Ω_{HI}	0.0024	0.0015	0.093	0.047	0.0038
10% b_{HI} & Ω_{HI}	0.0029	0.0018	0.11	0.065	0.0040

Broadband shape + massive neutrinos

CMB S4 + Euclid + Ext-HIRAX

Ext-HIRAX Σm_ν[eV]						
	$k_{\max} = 0.2h\text{Mpc}^{-1}$			$k_{\max} = k_{\text{nl}}(z)$		
Euclid No Rec.+PlanckBAO	0.050			0.049		
+21cm	No wedge	Mid wedge	Wedge	No wedge	Mid wedge	Wedge
2% b_{HI} & Ω_{HI}	0.037	0.038	0.045	0.030	0.031	0.040
2% b_{HI} & Ω_{HI}, diff $M_{\min}$	0.037	0.038	0.044	0.028	0.029	0.039
2% b_{HI} & Ω_{HI}, 1-loop	0.038	0.039	0.046	0.035	0.035	0.042
5% b_{HI} & Ω_{HI}	0.042	0.043	0.048	0.034	0.035	0.043
10% b_{HI} & Ω_{HI}	0.044	0.045	0.049	0.035	0.036	0.044
Euclid No Rec.+CMB-S4	0.031			0.030		
+21cm	No wedge	Mid wedge	Wedge	No wedge	Mid wedge	Wedge
2% b_{HI} & Ω_{HI}	0.022	0.022	0.028	0.018	0.018	0.025
2% b_{HI} & Ω_{HI}, diff $M_{\min}$	0.021	0.021	0.028	0.017	0.017	0.024
2% b_{HI} & Ω_{HI}, 1-loop	0.023	0.023	0.028	0.020	0.020	0.025
5% b_{HI} & Ω_{HI}	0.023	0.023	0.028	0.018	0.019	0.025
10% b_{HI} & Ω_{HI}	0.023	0.023	0.028	0.019	0.019	0.025

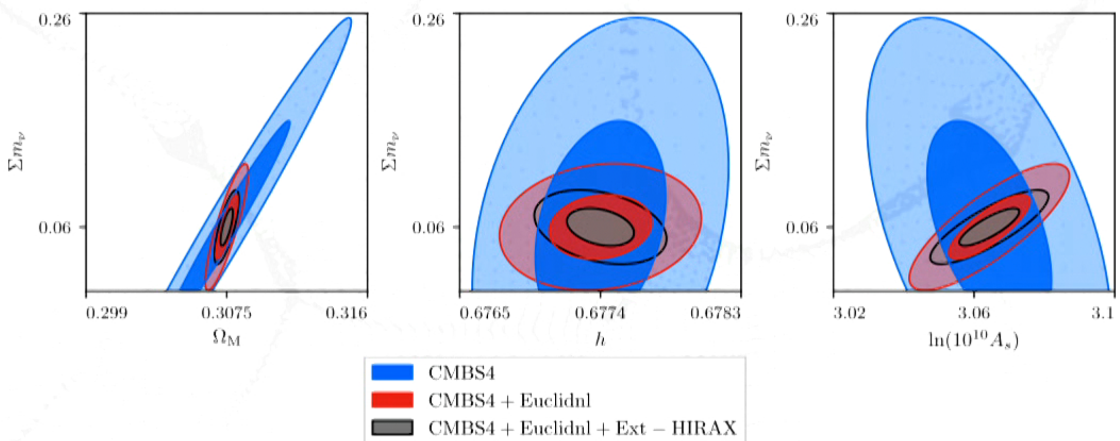

Neutrino masses uncertainty — τ prior

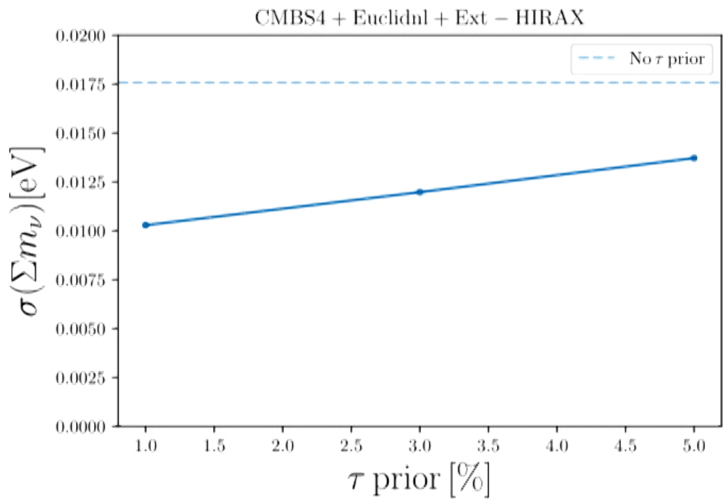

Breaking the degeneracy $\Sigma m_\nu - w$

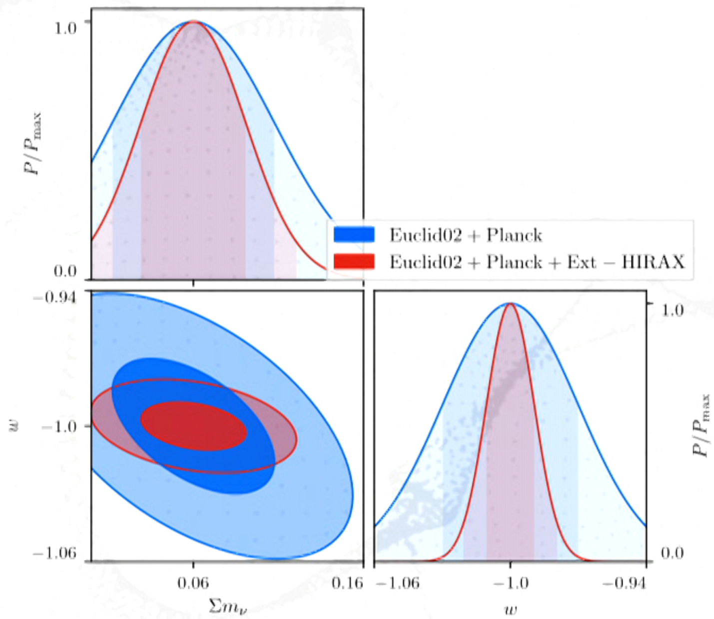

Main conclusions

- We investigate the possibility of performing cosmological studies in the redshift range $2.5 < z < 5$ through suitable extensions of existing and upcoming radio-telescopes like CHIME, HIRAX and FAST.
- We use Fisher formalism to forecast tight constraints on growth parameter fs8 (4%) and AP parameters (1%) as a function of redshift in narrow redshift bins dz=0.1.
- In combination with data from Euclid-like galaxy surveys and CMB S4, the sum of the neutrino masses can be constrained with an error equal to 23 meV (1σ), while Neff can be constrained within 0.02 (1σ).
- We study in detail the dependence of our results on the instrument, amplitude of the HI bias, the foreground wedge coverage, the non-linear scale used in the analysis, uncertainties in the theoretical modelling and the priors on bHI and ΩHI.

Cosmic Visions 21cm Collaboration:

Inflation and Early Dark Energy with a Stage II Hydrogen IM experiment

arXiv:1810.09572

- This white paper envisions a revolutionary post-DESI, post-LSST dark energy program based on IM of the redshifted 21 cm emission line from HI out to redshift z ~ 6 at radio frequencies. The proposed IM survey has the unique capability to quadruple the volume of the Universe surveyed by optical programs, provide a percent-level measurement of the expansion history to z ~ 6, open a window to explore physics beyond the concordance ΛCDM model, and to significantly improve the precision on standard cosmological parameters.

- In addition, characterization of dark energy and new physics will be powerfully enhanced by cross-correlations with optical surveys and cosmic microwave background measurements. The rich dataset obtained by the proposed IM instrument will be simultaneously useful in exploring the time-domain physics of fast radio transients and pulsars, potentially in live "multi-messenger" coincidence with other observatories.

- The core Dark Energy/Inflation science advances enabled by this program are the following:
  i) Measure the expansion history of the universe in the pre-acceleration era at the same precision as at lower redshifts, providing an unexplored window for new physics.
  ii) Observe, or constrain, the presence of inflationary relics in the primordial power spectrum, improving existing constraints by an order of magnitude;
  iii) Observe, or constrain, primordial non-Gaussianity with unprecedented precision, improving constraints on several key numbers by an order of magnitude.

Cosmic Visions 21cm Collaboration:
Inflation and Early Dark Energy with a Stage II Hydrogen IM experiment

arXiv:1810.09572

Overview: Stage II 21cm intensity mapping survey

- Large-volume cosmological survey optimized for BAO and bispectrum science, covering half the sky at $z = 2 - 6$.
- Main science goals:
  - Expansion history and physics of dark energy in pre-acceleration era
  - Inflationary features in primordial power spectrum
  - Non-Gaussianity of primordial power spectrum
- Reference design:
  - Compact array of 256×256 dishes of 6m diameter, using FFT correlation and redundant calibration.
  - Room-temperature dual-polarization receivers, covering $200 - 500$ MHz.
- 5 years on-sky time, targeted at project start ~ 2025

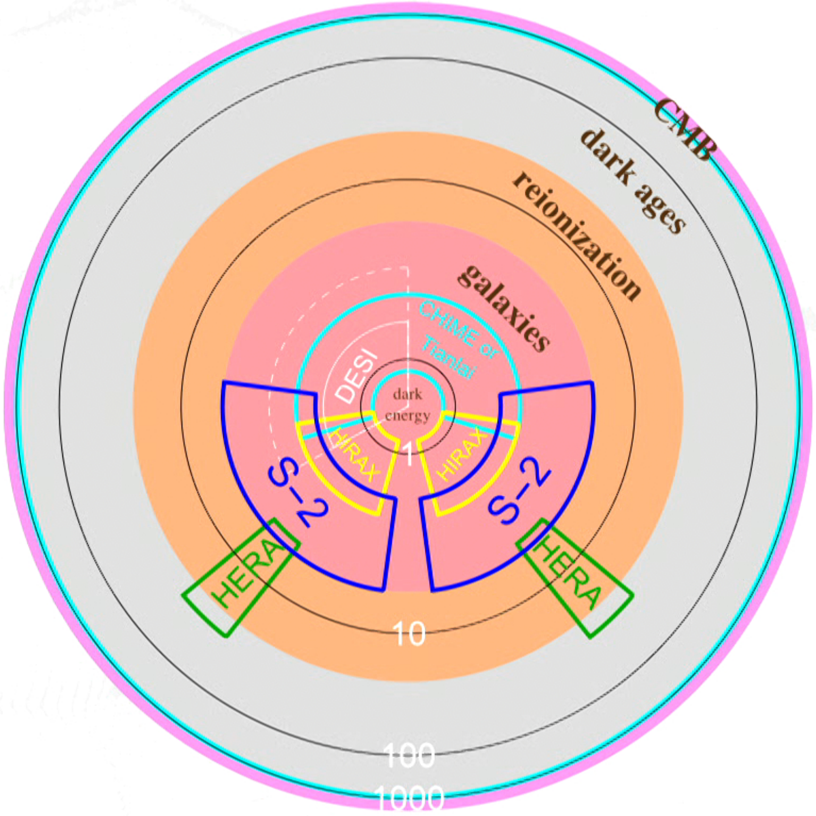

The HI content of dark matter haloes at $z \approx 0$ from ALFALFA

with D. Alonso, F. Villaescusa-Navarro, I. Yoon & M. Jones

arXiv:1805.00934

Arecibo Legacy Fast ALFA (ALFALFA)

- Blind extragalactic HI survey using Arecibo to probe the local HI Universe
- Provides measurements of positions, velocities, fluxes and line widths of HI sources
- More than 30,000 extragalactic HI sources to z≈0.06, 7000 deg^2
- We use this data to combine clustering + groups catalog from SDSS + Ω_{HI} measurements in order to constrain the M_{HI}-M_h relation

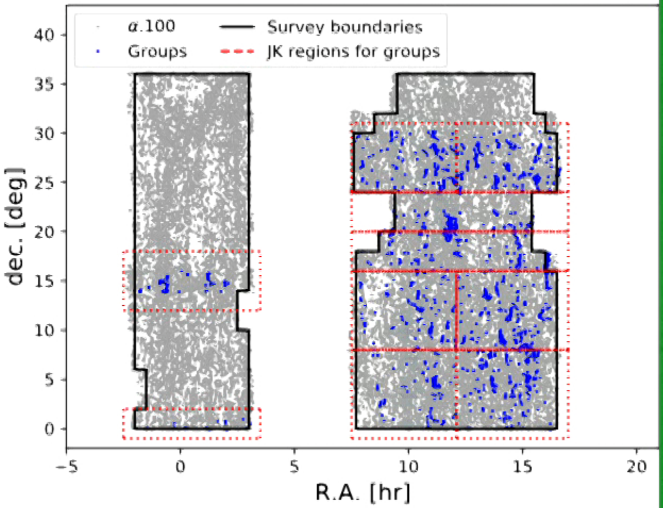

The projected 2-point correlation function

We use the Landy & Szalay estimator for the 2D 2PCF:

$$\xi(\pi,\sigma) = \frac{\mathrm{DD}(\pi,\sigma) - 2\mathrm{DR}(\pi,\sigma) + \mathrm{RR}(\pi,\sigma)}{\mathrm{RR}(\pi,\sigma)}$$

with

$$\mathrm{DD}(\pi,\sigma) = \frac{\sum_{i=1}^{N}\sum_{j>i} w_i w_j \Theta\left(\pi_{ij};\pi,\Delta\pi\right)\Theta\left(\sigma'_{ij};\sigma,\Delta\sigma\right)}{\sum_{i=1}^{N}\sum_{j>i} w_i w_j}$$

and use FKP + M_{HI} weights:

$$w_i = \frac{m_{\mathrm{HI,i}}}{1 + 4\pi n\left(d_i\right) J_3\left(r_{ij}\right)} \qquad J_3(r) = \int_0^r r^2 \xi\left(r'\right) dr'$$

Finally we project along the line of sight to obtain:

$$\Xi(\sigma) = \int_{-\infty}^{\infty} d\pi \xi(\sigma,\pi) \simeq 2\sum_{0}^{\pi_{\max}} \xi(\sigma,\pi)\Delta\pi$$

We model it using the HI halo model:

$$\Xi(\sigma) = \int_0^{\infty} \frac{kdk}{2\pi}\left[P_{\mathrm{HI,1h}}(k) + P_{\mathrm{HI,2h}}(k)\right] J_0(k\sigma)$$

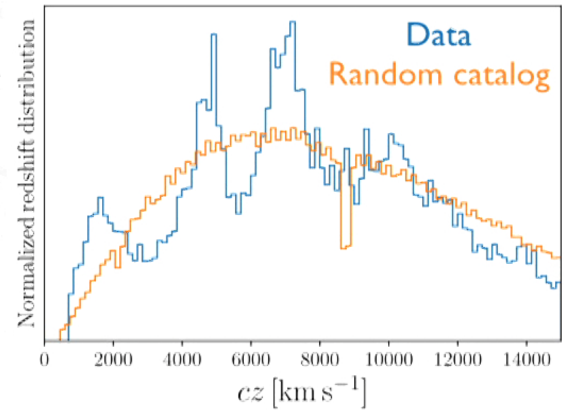

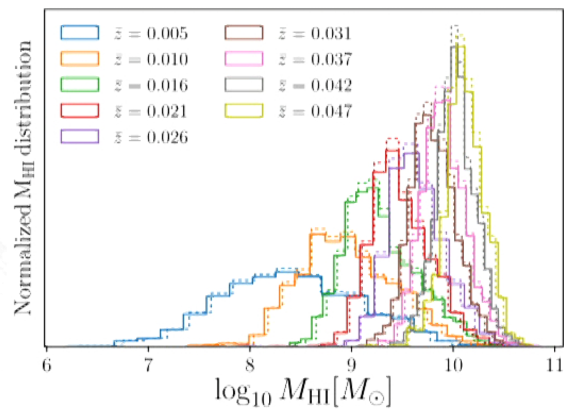

The projected 2-point correlation function

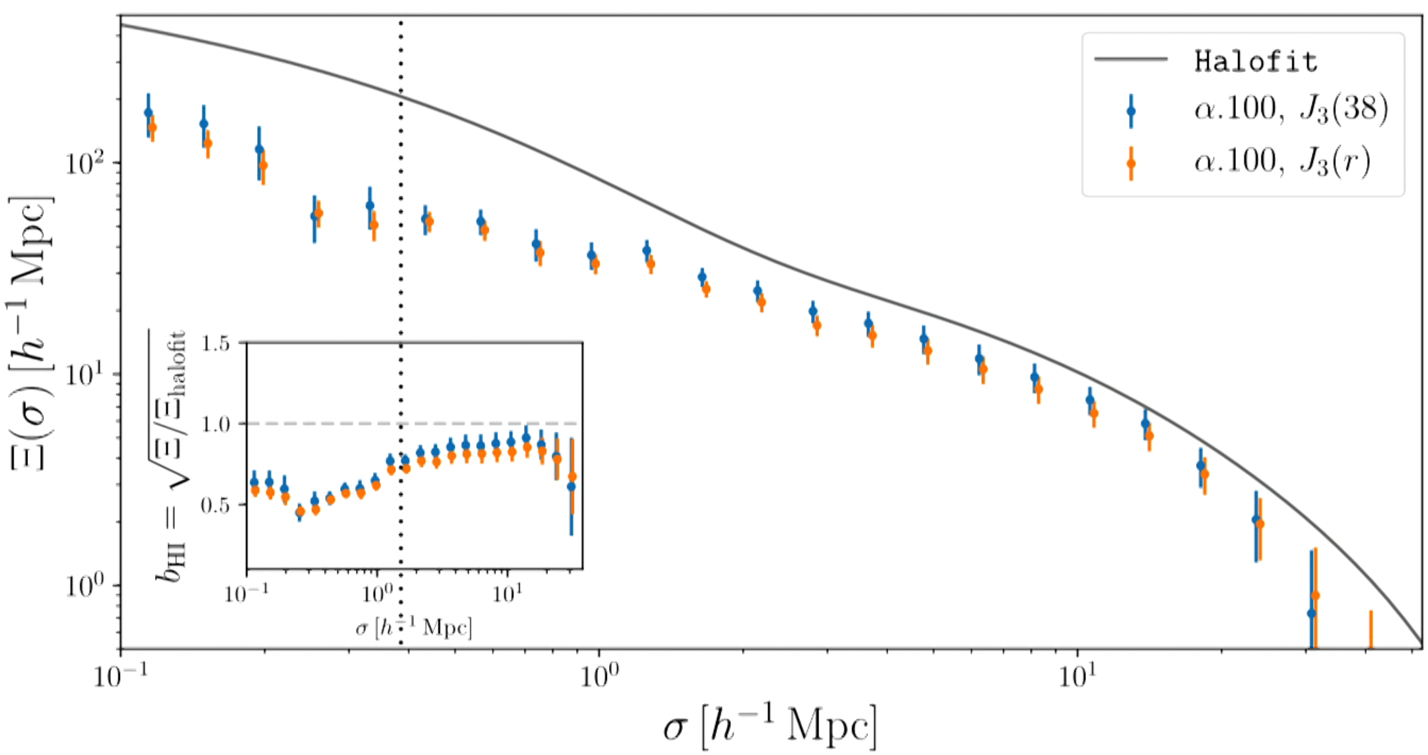

HI content in groups

1. We separate SDSS group catalog into 7 log-spaced halo mass bins

2. In each bin we estimate the HI mass function using the 2D step-wise maximum likelihood (2DSWML) estimator

3. To extrapolate bellow the detection limit we model each HI m.f. as a Schechter function:

$$\phi\left(m_{\rm HI}\right) = \ln(10)\phi_* \left(\frac{m_{\rm HI}}{M_*}\right)^{\alpha_s+1} \exp\left(-\frac{m_{\rm HI}}{M_*}\right)$$

4. We integrate over reconstructed HI m.f. to recover the corresponding total HI mass

5. We also integrate the HI m.f. directly over the available range of HI masses to check for systematics
6. Finally, we use rescaled best-fit HI m.f. found for the complete ALFALFA catalog

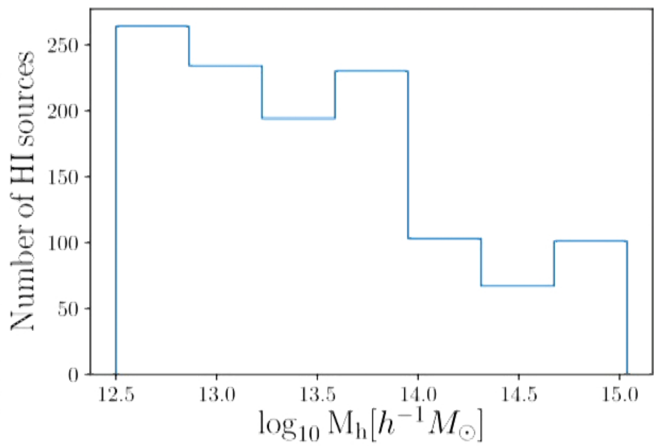

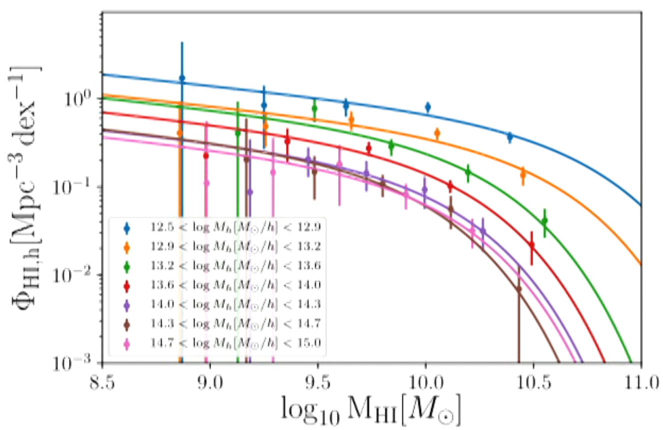

HI content in groups

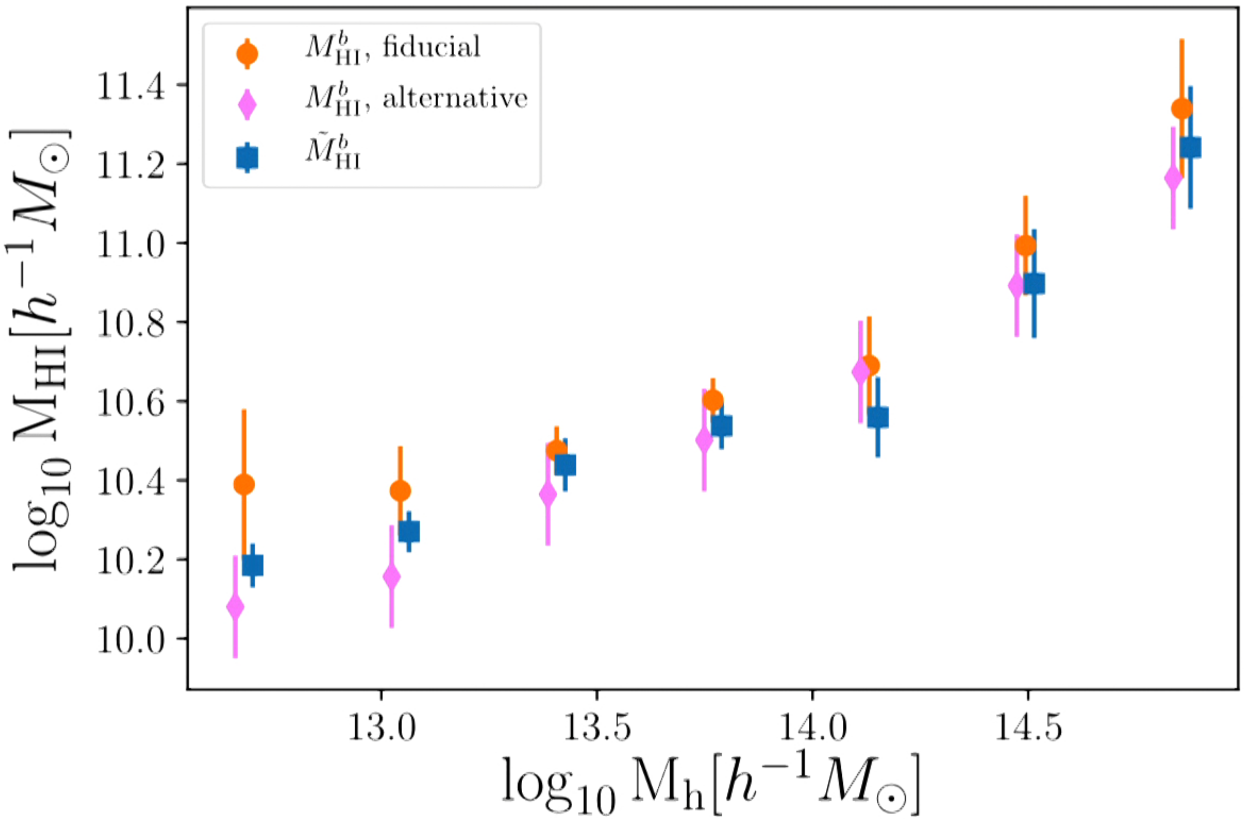

Results

$$M_{\rm HI}(M) \propto e^{-M_{\rm min}/M} M^{\alpha}$$

$$\theta = \{M_0, M_{\rm min}, \alpha, c_{\rm HI,0}\}$$

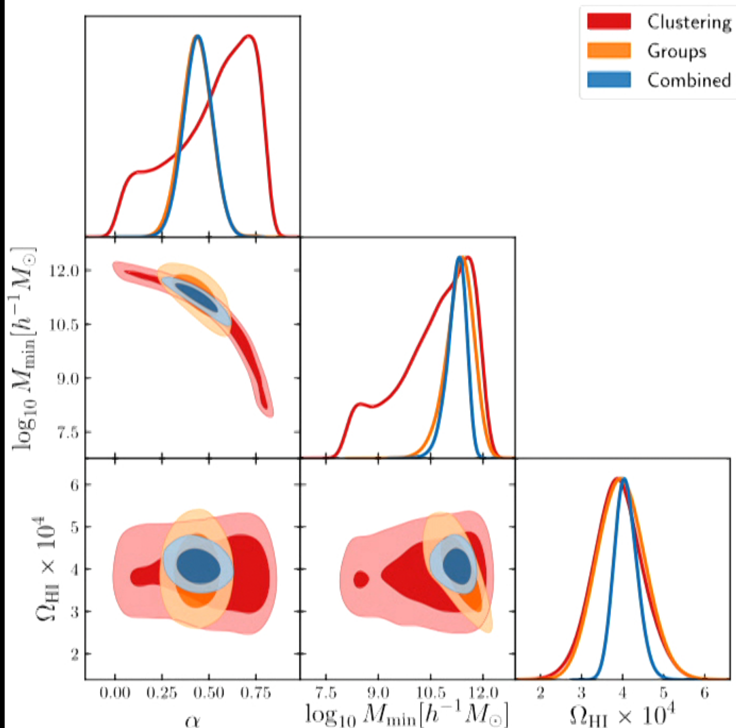

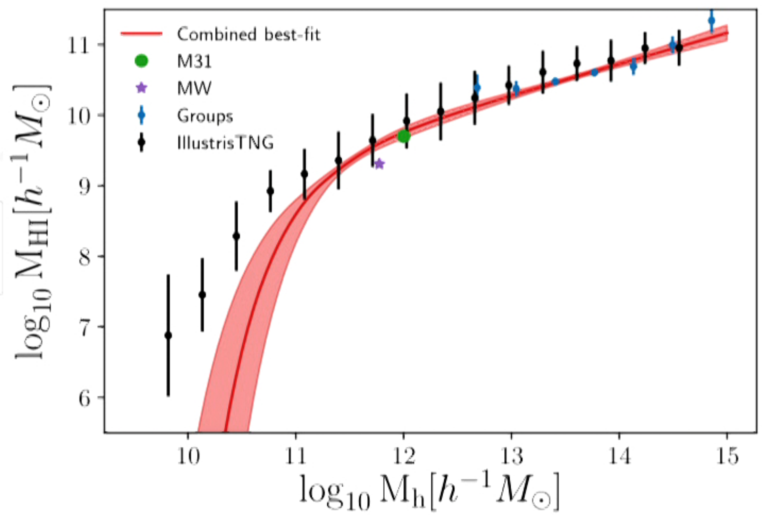

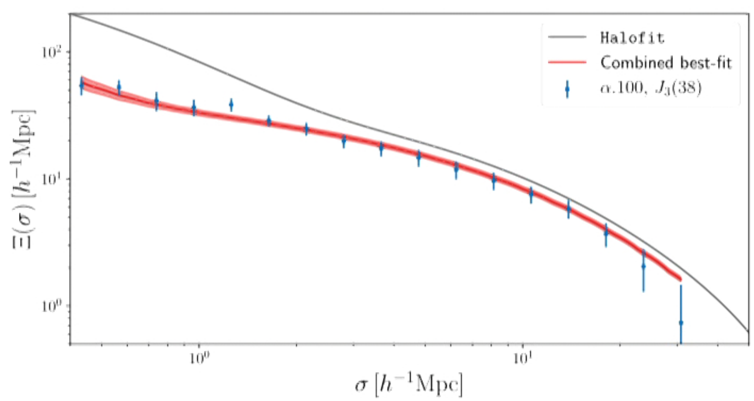

Prediction on HI bias and shot-noise

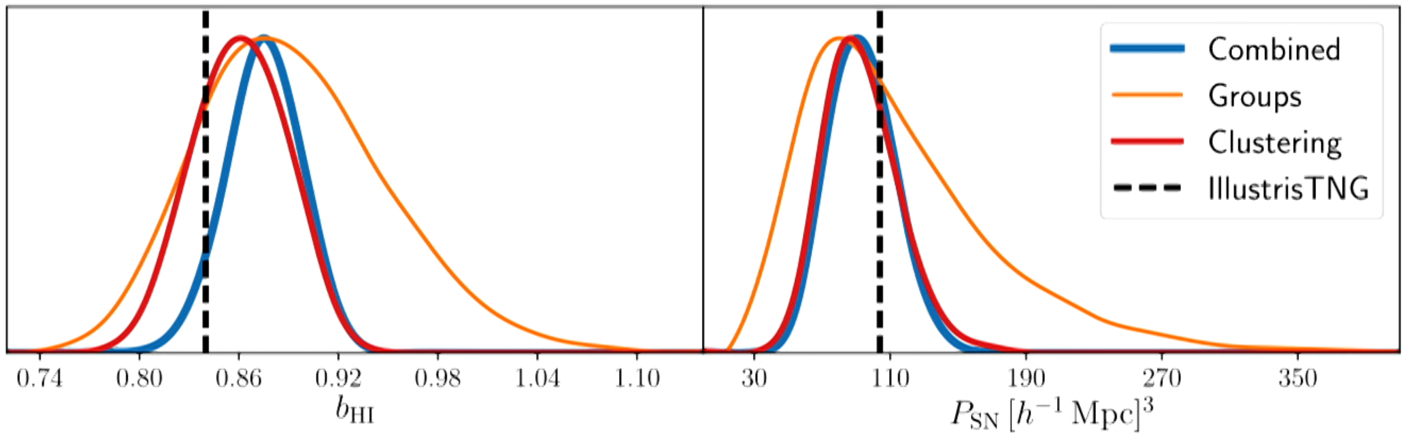

Main conclusions

- We have used the HI-weighed clustering of 21cm sources detected by ALFALFA plus the abundance of those sources in halos identified in the galaxy group catalog compiled from the SDSS DR7 data.
- We used a halo-model-based approach to model the abundance and clustering of HI by parametrizing the $M_{HI}(M_h)$ relation as a power law with an exponential mass cutoff.
- We place constraints on the distribution of HI in DM halos as a function of halo mass.
- We find datasets to be consistent in derived parameters and also in agreement with the state-of-the-art magneto-hydrodynamical simulations.
- We make a prediction for the HI bias and the HI shot-noise at z=0.
- The clustering properties of the HI derived in this work are a very relevant piece of information for future 21cm IM studies.

Summary

- I have been mostly focussed on using post-reionization HI as the LSS probe through 21cm IM, but the tools are almost the same as for the galaxy clustering.

- In brief we have:

  - developed and studied in detail using numerical simulations a method to reconstruct the BAO peak with future 21cm IM;

  - studied the gains of performing 21cm IM surveys at vastly unexplored redshift ranges $2.5<z<5$ through Fisher matrix formalism;

  - constrained the content of HI in halos using data at z=0 from HI survey and group catalog of optical galaxies giving us a prediction of the HI bias and shot-noise.

- We believe most of this work could be useful for future 21cm IM studies.

Future work

Mainly working on DESI Galaxy Clustering measurements and pipeline with Will Percival

Open to LSS/21cm side projects

Happy to collaborate and help!